Measurements of $|V_{cb}|$ and $|V_{ub}|$ status and prospects at LHCb

LHCb implications workshop
October 2023

Veronica S. Kirsebom, on behalf of the LHCb Collaboration

Flavour changing transitions in the quark sector

$$\begin{pmatrix} d' \\ s' \\ b' \end{pmatrix} = \begin{pmatrix} V_{ud} & V_{us} & V_{ub} \\ V_{cd} & V_{cs} & V_{cb} \\ V_{td} & V_{ts} & V_{tb} \end{pmatrix} \begin{pmatrix} d \\ s \\ b \end{pmatrix}$$

- CKM matrix elements are **fundamental parameters.**

  → Precise determinations are important.

- $|V_{cb}|$ and $|V_{ub}|$ represent a **long-standing puzzle.**

  → Complementary methods yield inconsistent results.

  → Limits their precision.

- **We need to know $|V_{cb}|$ and $|V_{ub}|$ precisely to constrain the Unitary Triangle of the CKM matrix.**

[CKMfitter Group, the global CLM fit (2021)]

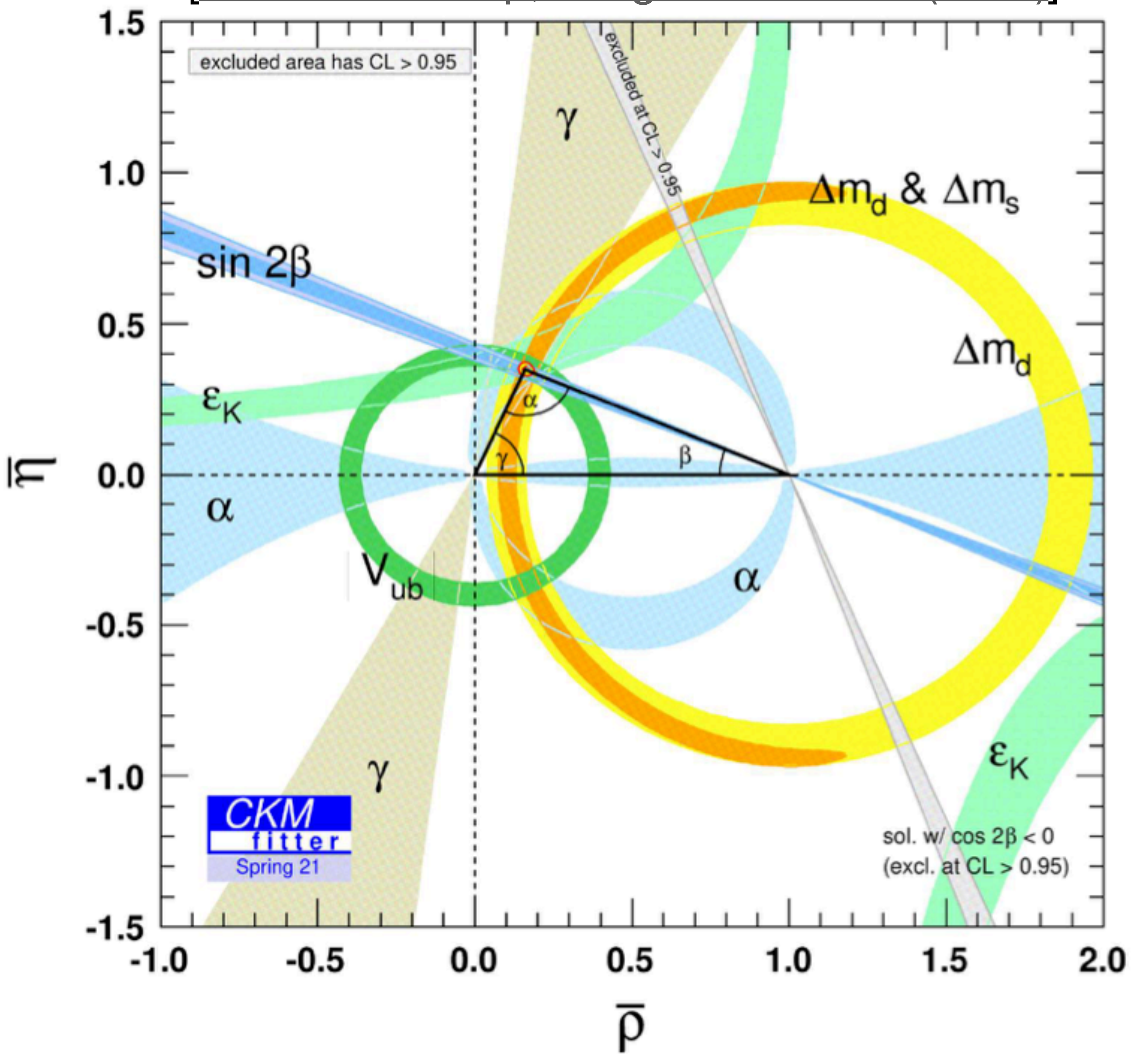

Determining the $|V_{cb}|$ and $|V_{ub}|$ matrix elements

- Usually, done with **semileptonic decays** $X_b \to X_{c,u} l\nu$.

→ **Theoretically clean**
(only one hadronic current).

→ **Experimentally feasible**
(large enough BFs).

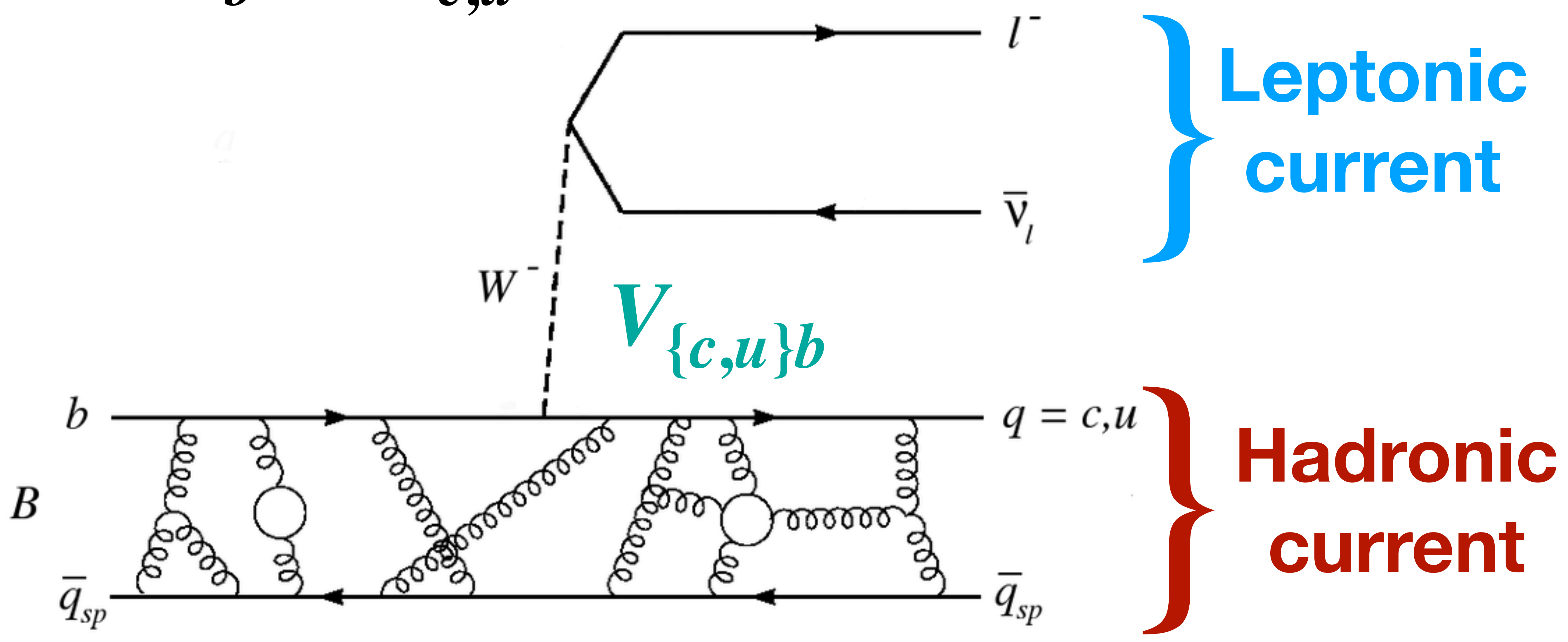

Leptonic $B \to l\nu$ decays are theoretically simpler, but experimentally much harder.

→ only on signal track and small BFs.

Described by form factors (FFs) :

→ Functions $q^2 = (p_\mu + p_\nu)^2$.

→ Calculated with num-methods:
LCSR (small q^2) or LQCD (high q^2).

Two complementary methods to determine $|V_{cb}|$ and $|V_{ub}|$

- **Exclusive** and **inclusive** semileptonic $X_b \rightarrow X_{c,u} l\nu$ decays.

  → Largely theoretically and experimentally independent.

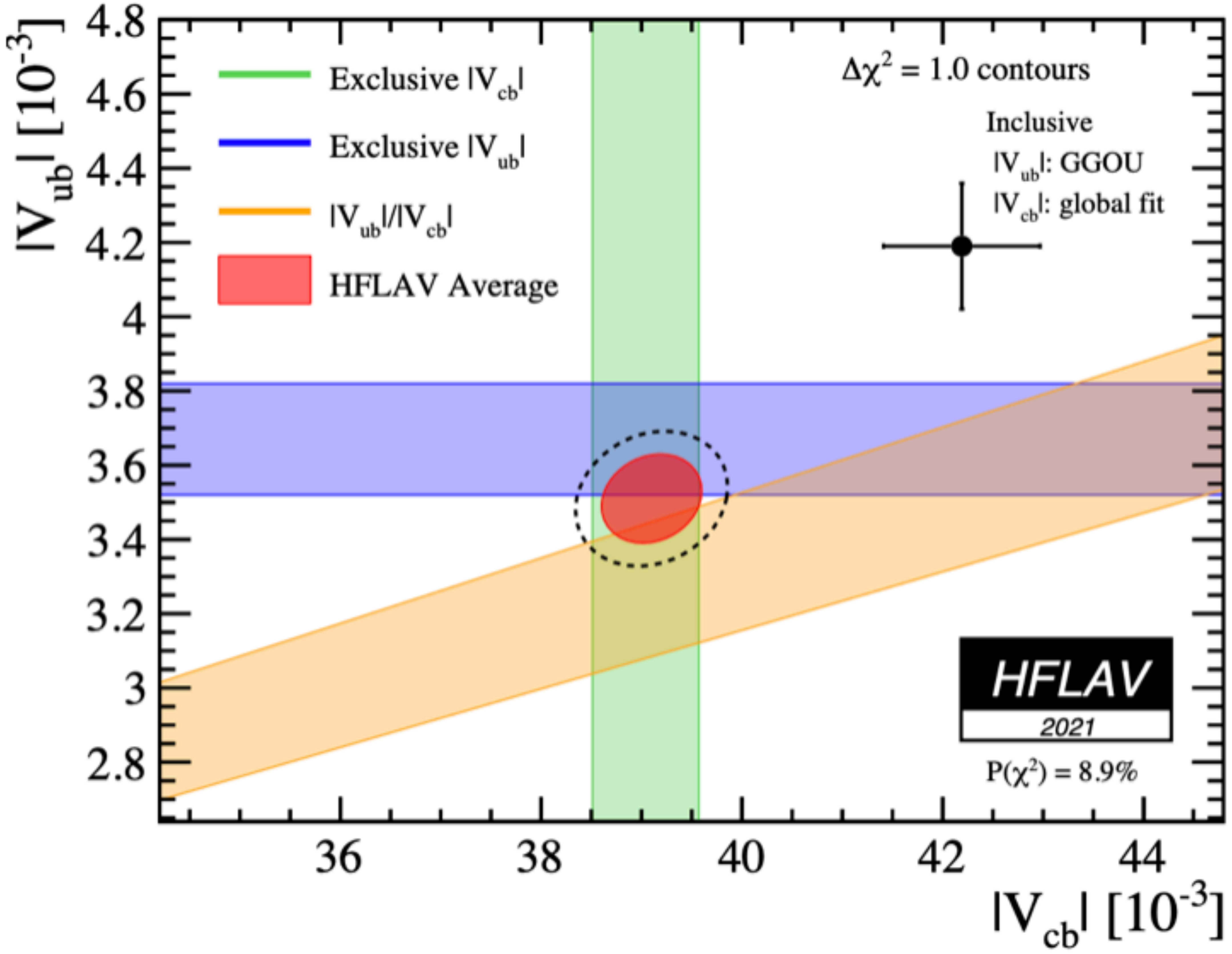

→ **Long-standing tension** ($\sim 3\sigma$).

→ **Limits the precision of SM tests and sensitivity to NP.**

[Phys. Rev. D 107, 052008 (2023)]

Measuring $|V_{cb}|$ and $|V_{ub}|$ at LHCb

- @ LHCb, **exclusive semileptonic decays** can be measured (inclusive semileptonic decays are measured at the B factories).

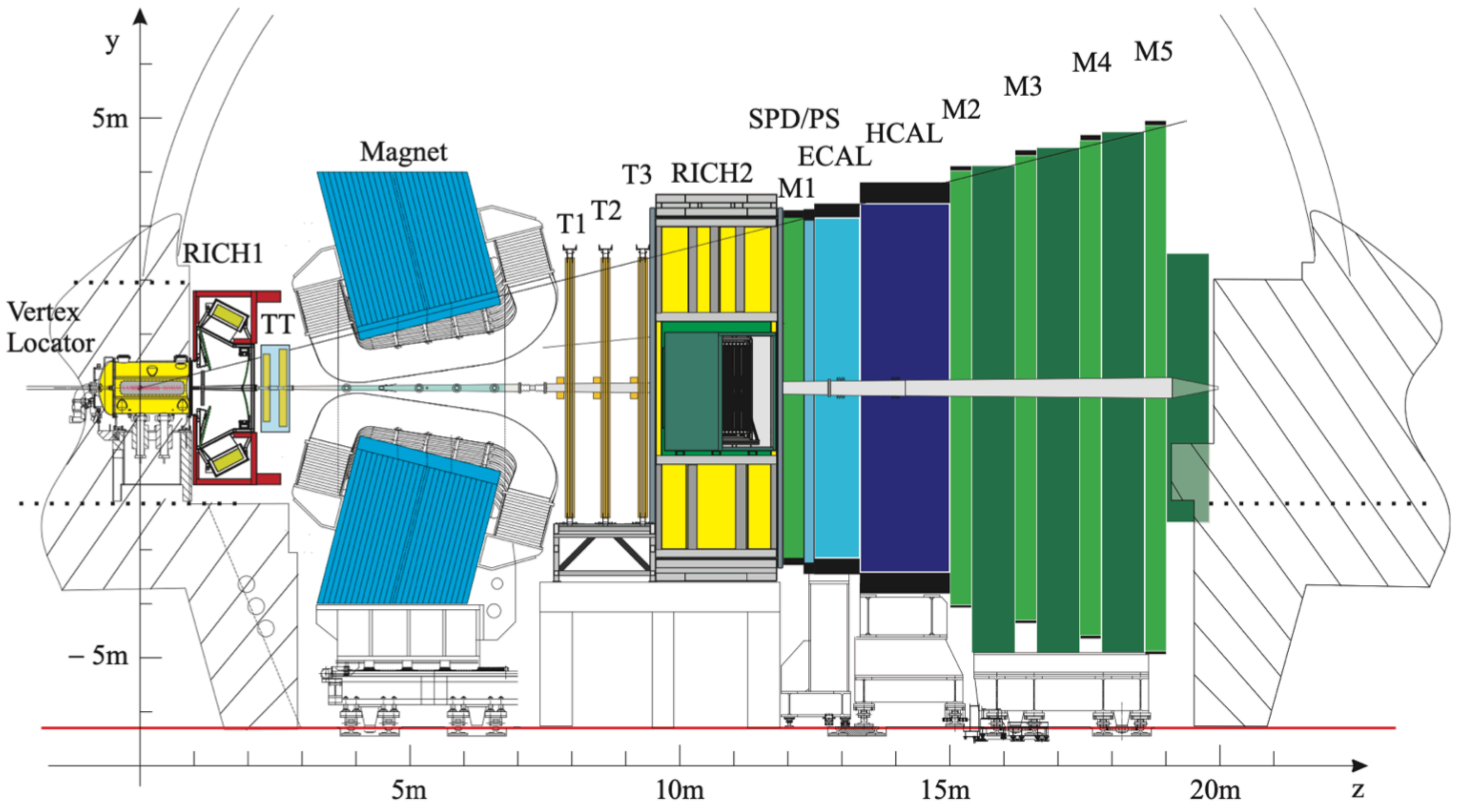

[Int. J. Mod. Phys. A 30 (2015), 1530022]

Pros @ LHCb:

- **Large samples** of $B^{\pm,0}$ mesons as well as heavier b hadrons including B_s^0, B_c and Λ_b^0.

Cons @ LHCb:

- Hadronic environment and unreconstructed ν → **large backgrounds**.
- The $b\bar{b}$ production rate cannot be determined precisely → **large uncertainty of measured BFs.**

Some ingredients for semileptonic analyses at LHCb

Corrected mass [Phys.Rev.Lett.80:660-665,(1998)]:

$$m_{\text{corr}}(X_b) = \sqrt{m(X_q l)^2 + p_\perp(X_q l)^2} + p_\perp(X_q l)$$

→ Discriminating variable corrects for missing ν.

$X_b \to X_{q=\{c,u\}} l \nu$

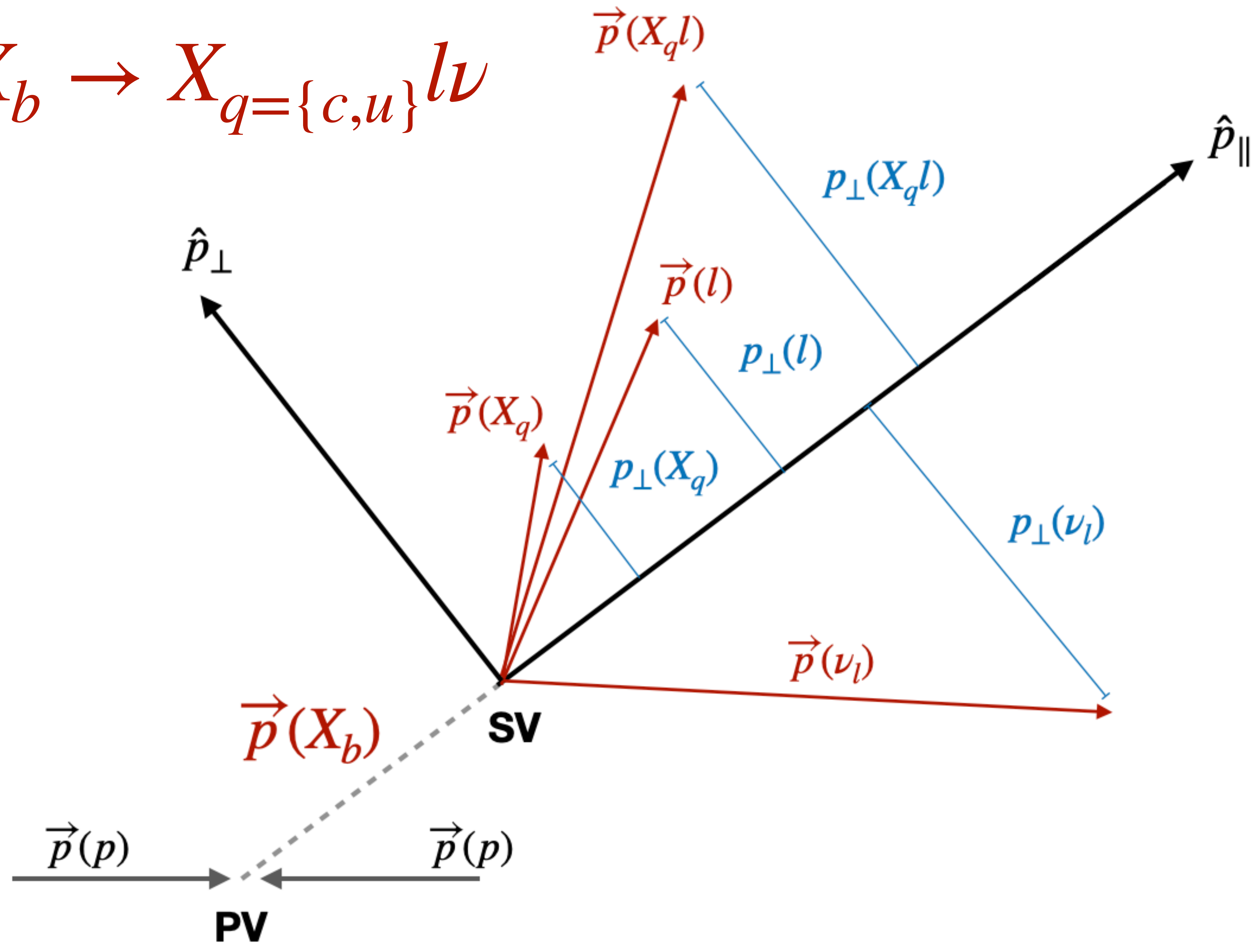

Determining q^2 up to a two-fold ambiguity.

→ degraded q^2 resolution.

→ Unfolding required to obtain the true q^2.

Normalisation decays used to cancel $b\bar{b}$-production uncertainties.

→ External inputs: e.g. normalisation BFs, fragmentation fractions etc.

Measurement of $|V_{cb}|$ from the $B_s^0 \to D_s^{(*)-}\mu^+\nu_\mu$ decay [Phys. Rev. D 101 (2020)]

>> First $|V_{cb}|$ extraction from a B_s^0 decay.

- **Dataset:** 1.0 fb^{-1} @ $\sqrt{s} = 7$ TeV and 2.0 fb^{-1} @ $\sqrt{s} = 8$ TeV (Run 1, 2011& 2012).
- **Signal:** $B_s^0 \to D_s^{(*)-}\mu^+\nu_\mu$.
- **Normalisation:** $B^0 \to D^{(*)-}\mu^+\nu_\mu$.

→ For both channels, $D^-_{(s)}$ is reconstructed in the $[K^+K^-]_\phi\pi^-$ final state.

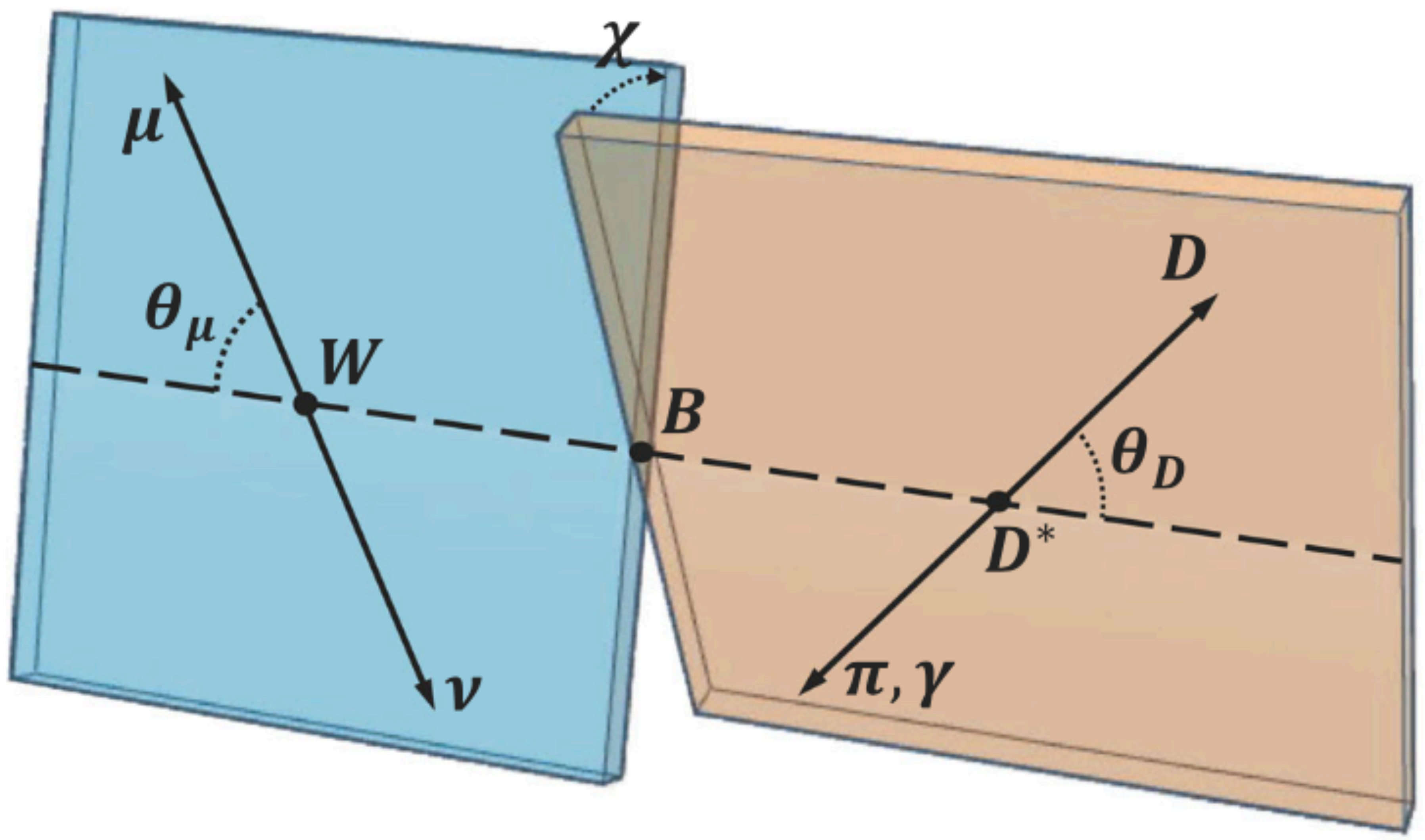

- Differential decay rates ($m_\mu \approx 0$):

$$\frac{d\Gamma(B_s^0 \to D_s^-\mu^+\nu_\mu)}{dw} = \frac{G_F^2 m_D^3}{48\pi^3}(m_B + m_D^2)^2\eta_{EW}^2 \times |V_{cb}|^2 (w^2-1)^{3/2}|G(w)|^2$$

One FF

$$\frac{d^4\Gamma(B_s^0 \to D_s^{*-}\mu^+\nu_\mu)}{dw\, d\cos\theta_\mu d\cos\theta_D d\chi} = \frac{3G_F^2 m_{B_s^0}^3 m_{D_s^*}^2}{16(4\pi)^4}\eta_{EW}^2 \times |V_{cb}|^2 |A(w,\theta_\mu,\theta_D,\chi)|^2$$

Three FFs

Where $w = v_{B_s^0} \times v_{D_s^{(*)-}}$ is the hadronic recoil variable that depends on q^2 and θ_D, θ_μ and χ are the three helicity angles:

FFs can be modelled with the parameterisations:

CLN: Caprini, Lellouch and Neubert [Nucl. Phys. B530 (1998) 153]

BGL: Boyd, Grinstein and Lebed [Phys. Rev. Lett. 74 (1995) 4603]

→ Differential measurements allow us to extract information on the FFs.

Measurement of $|V_{cb}|$ from the $B_s^0 \to D_s^{(*)-}\mu^+\nu_\mu$ decay [Phys. Rev. D 101 (2020)]

>> Alternative method to infer FFs.

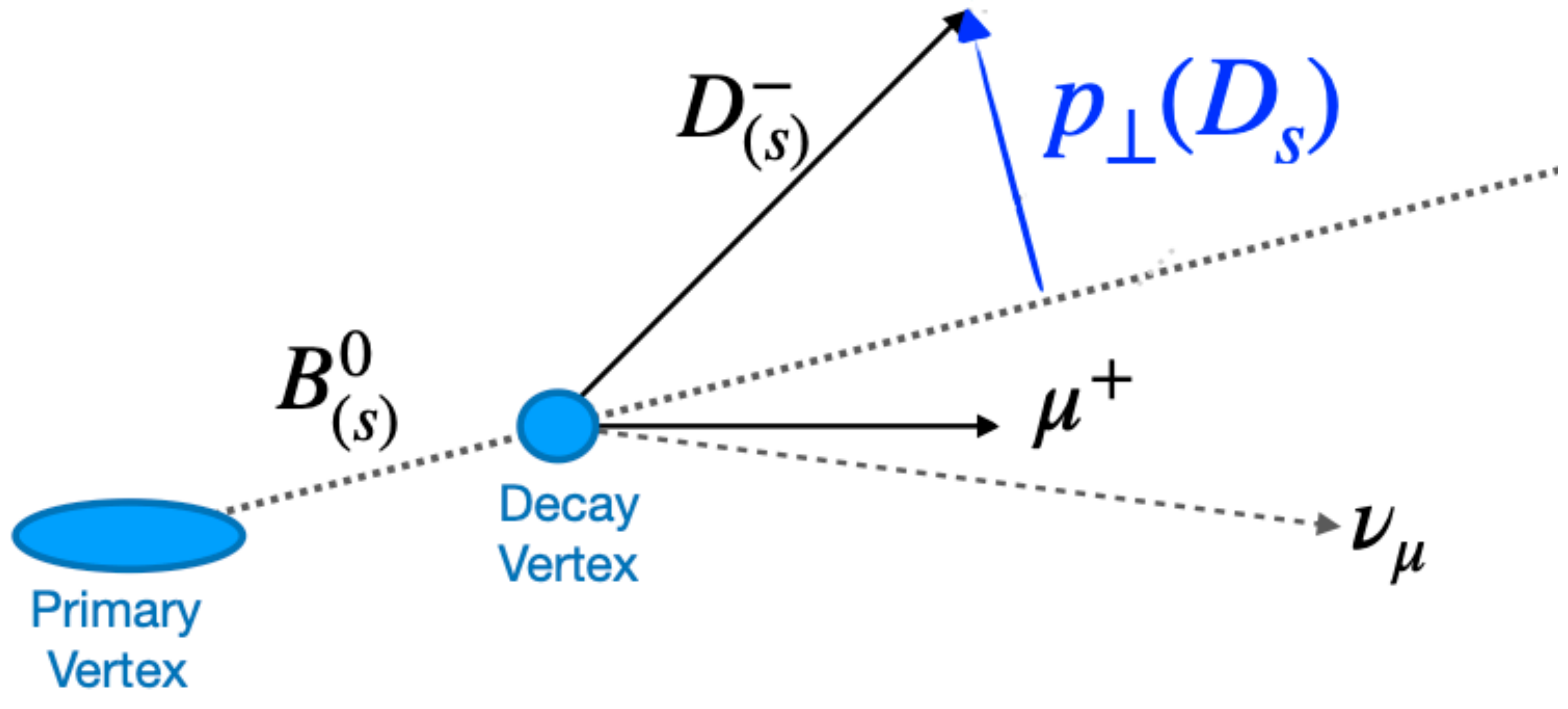

- Usually, FFs are extracted by measuring the decay distribution wrt. q^2 or $w = w(q^2)$.
- This analysis exploits a new variable, $p_\perp(D_s^-)$, which is an approximation of w.

→ **Strongly correlated with** w, and thus, with the FFs.

→ Can be **fully reconstructed**.

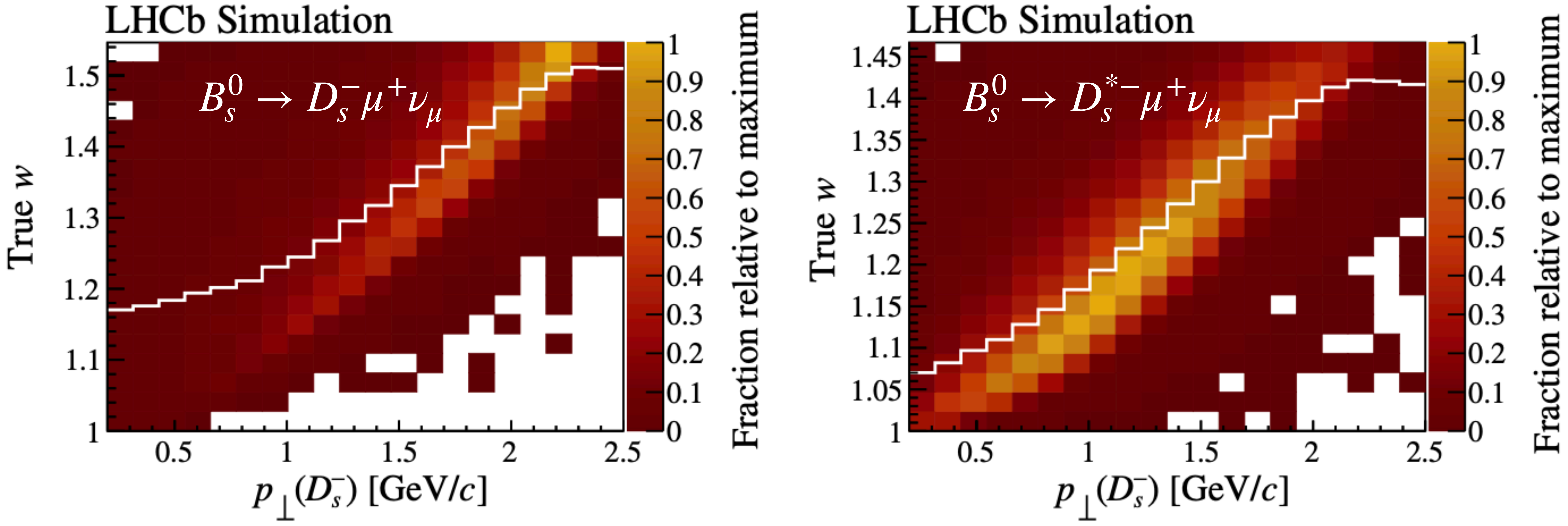

Measurement of $|V_{cb}|$ from the $B_s^0 \to D_s^{(*)-}\mu^+\nu_\mu$ decay [Phys. Rev. D 101 (2020)]

- **Signal** and **normalisation yields** are determined in fits to m_{corr}- $p_\perp(D_s^-)$.

- To determine $|V_{cb}|$ and **FFs** the **signal yields** are expressed as:

Signal fit with the **CLN** parameterisation

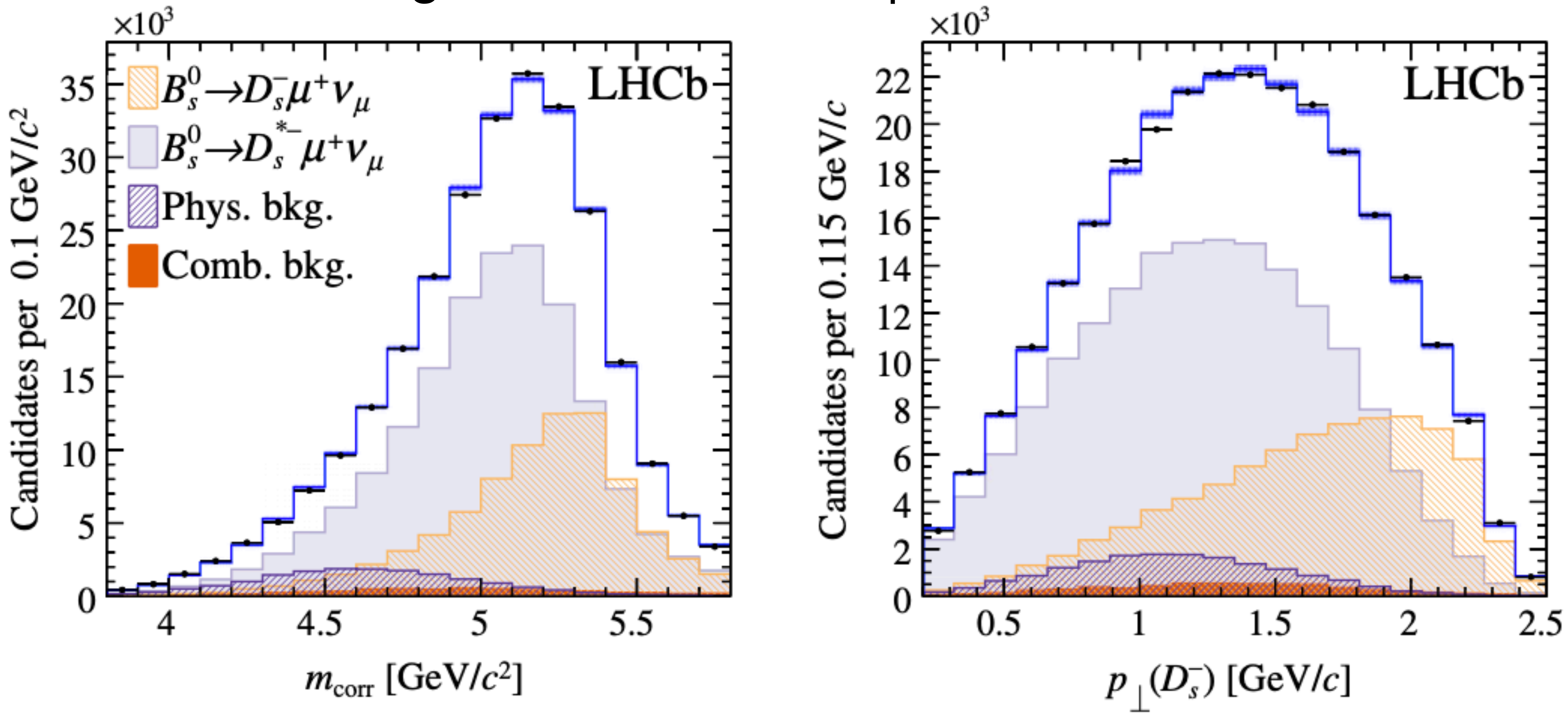

$$N_{sig}^{(*)} = \frac{N_{norm}^{(*)}}{BF_{norm}} \times \frac{f_s}{f_d} \times BF(D_s^- \to K^+K^-\pi^-) \times \tau_{B_s^0} \times R_\epsilon \times \int \frac{d\Gamma(B_s^0 \to D_s^{(*)-}\mu^+\nu_\mu)}{dx} dx$$

Normalisation yield ($N_{norm}^{(*)}$)

Normalisation BFs (BF_{norm}) [Phys. Rev. D 98, 030001 (2018)].

Product derived from LHCb measurement [Phys. Rev.D 100, 031102 (2019).] ($\frac{f_s}{f_d} \times BF(D_s^- \to K^+K^-\pi^-) \times \tau_{B_s^0}$)

signal/norm ratio of efficiencies (R_ϵ)

$|V_{cb}|$ and FFs ($\frac{d\Gamma}{dx}$)

$x = [w]$ for $B_s^0 \to D_s^- \mu^+ \nu_\mu$.

$x = [w, \theta_D, \theta_\mu, \chi]$ for $B_s^0 \to D_s^{*-} \mu^+ \nu_\mu$.

Measurement of $|V_{cb}|$ from the $B_s^0 \to D_s^{(*)-}\mu^+\nu_\mu$ decay [Phys. Rev. D 101 (2020)]

>> Final analysis result.

$$|V_{cb}|_{\mathrm{CLN}} = (41.4 \pm 0.6\,(\mathrm{stat}) \pm 0.9\,(\mathrm{syst}) \pm 1.2\,(\mathrm{ext})) \times 10^{-3}$$

$$|V_{cb}|_{\mathrm{BGL}} = (42.3 \pm 0.8\,(\mathrm{stat}) \pm 0.9\,(\mathrm{syst}) \pm 1.2\,(\mathrm{ext})) \times 10^{-3}$$

→ Measurements of CLN and BGL FF parameters are also reported.

- **CLN** and **BGL** extractions are compatible.
- Agree with previous exclusive and inclusive determinations.

Limitations on the $|V_{cb}|$ precision:

- **Uncertainty is dominated by external inputs:**

  → $f_s/f_d \times BF(D_s^- \to K^+K^-\pi^-)(\times\tau_{B_s})$ with $\sigma/|V_{cb}| \sim 2\,\%$.
  [Phys. Rev.D 100, 031102 (2019), Phys. Rev. Lett. 124, 122002 (2020)].

  → Normalisation BFs with $\sigma/|V_{cb}| \sim 2\,\%$.
  [Phys. Rev. D 98, 030001 (2018)].

- **Largest systematic uncertainty:**

  → $D_{(s)} \to K^+K^-\pi^-$ modelling with $\sigma/|V_{cb}| \sim 2\,\%$.

$\sigma(f_s/f_d)$ has been reduced with $\sim 50\,\%$ [Phys. Rev. D 104, 032005 (2021)].

→ Updated result will be shown later in this talk.

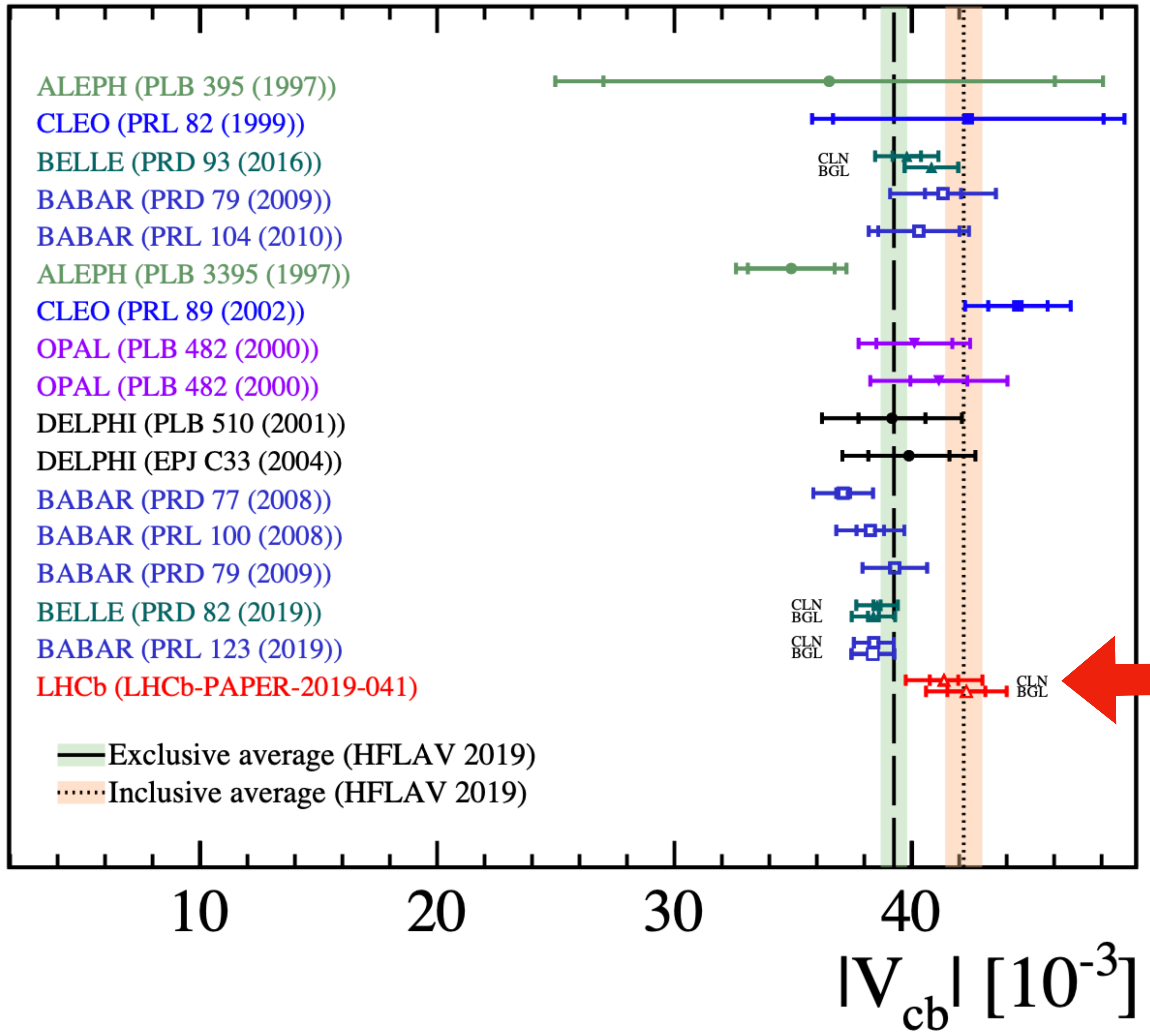

Measurement of the shape of the $B_s^0 \to D_s^{*-}\mu^+\nu_\mu$ differential decay rate

[J. High Energ. Phys. 144 (2020)]

- **Dataset:** 1.7 fb^{-1} @ $\sqrt{s} = 13$ TeV (Run 2, 2016).
- **Signal:** $B_s^0 \to D_s^{*-}(\to D_s^-\gamma)\mu^+\nu_\mu$.

  → γ is reconstructed in a cone around the D_s^-.

  → D_s^- reconstructed in $[K^+K^-]_\phi\pi^-$ and $[K^+\pi^-]_{K^{*0}}K^-$ final states.

- **Signal yields** are determined from fits to the $\boldsymbol{m_{\rm corr}(B_s^0)}$ distributions in **seven bins** of $\boldsymbol{w}_{\rm rec}$.
- $B_s^0 \to D_s^{*-}\mu^+\nu_\mu$ spectrum is unfolded in the **true** $\boldsymbol{w}$.
  1. Accounting for **detector resolution of** $\boldsymbol{w}$.
  2. Correcting for **reconstruction and selection efficiencies**.

- Unfolded spectrum is fitted with:

  CLN [Nucl. Phys. B530 (1998) 153]

  BGL [Phys. Rev. Lett. 74 (1995) 4603]

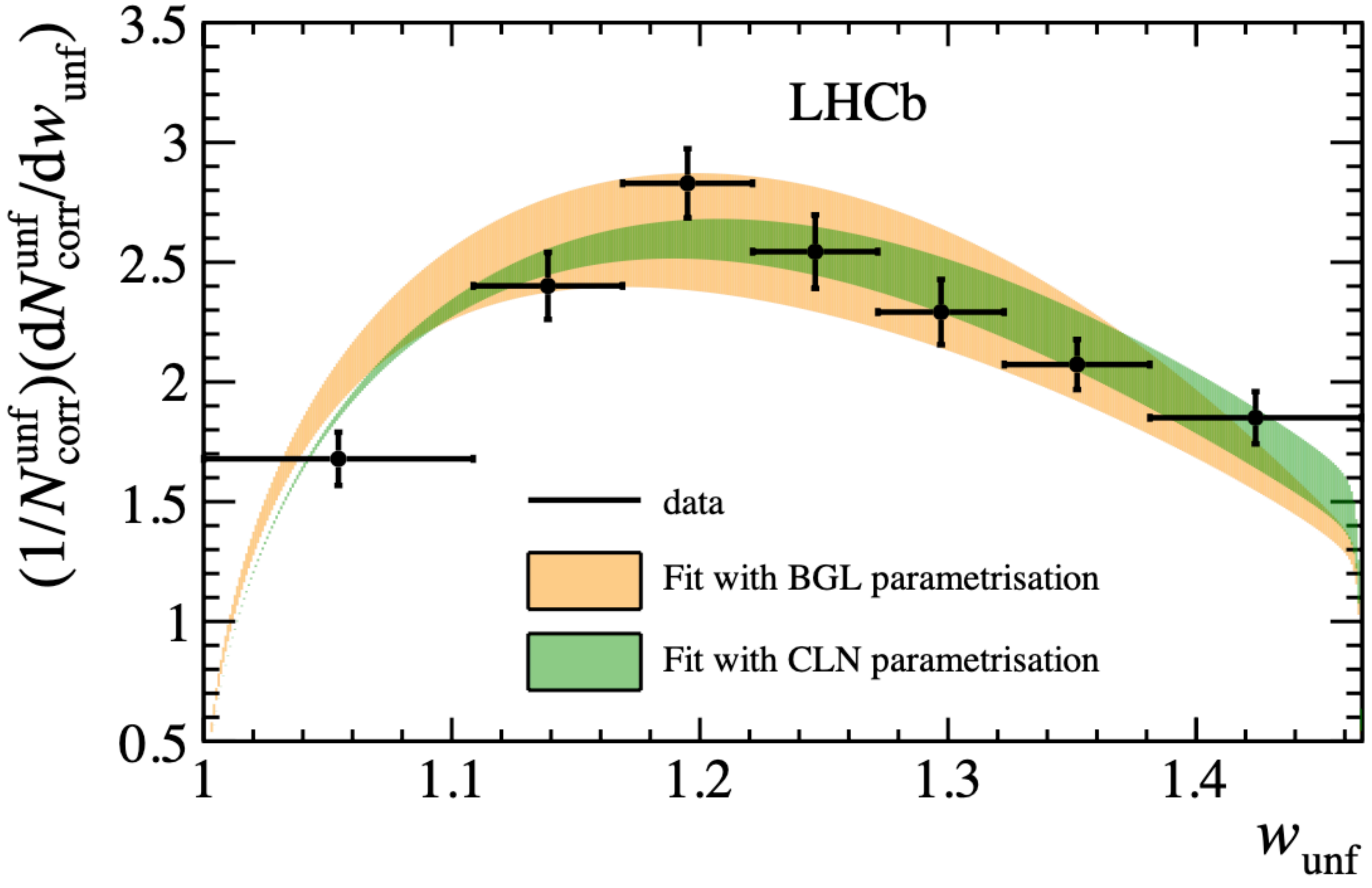

→ Both fits **give consistent results** and **describe the measured spectrum well.**

→ Results allows to **constrain FF parameterisations.**

Measuring $|V_{ub}|$ from the $\Lambda_b^0 \to p^+\mu^-\bar{\nu}_\mu$ decay [Nature Physics 11 (2015)]

>> First $\Lambda_b^0 \to p^+\mu^-\bar{\nu}_\mu$ observation and $|V_{ub}|$ extraction from baryonic decay.

Dataset: $2.0\ \text{fb}^{-1}$ @ $\sqrt{s} = 8$ TeV (Run 1, 2012).

Signal: $\Lambda_b^0 \to p^+\mu^-\bar{\nu}_\mu$.

Normalisation: $\Lambda_b^0 \to \Lambda_c^+\mu^-\bar{\nu}_\mu$ with $\Lambda_c^+ \to pK^-\pi^+$.

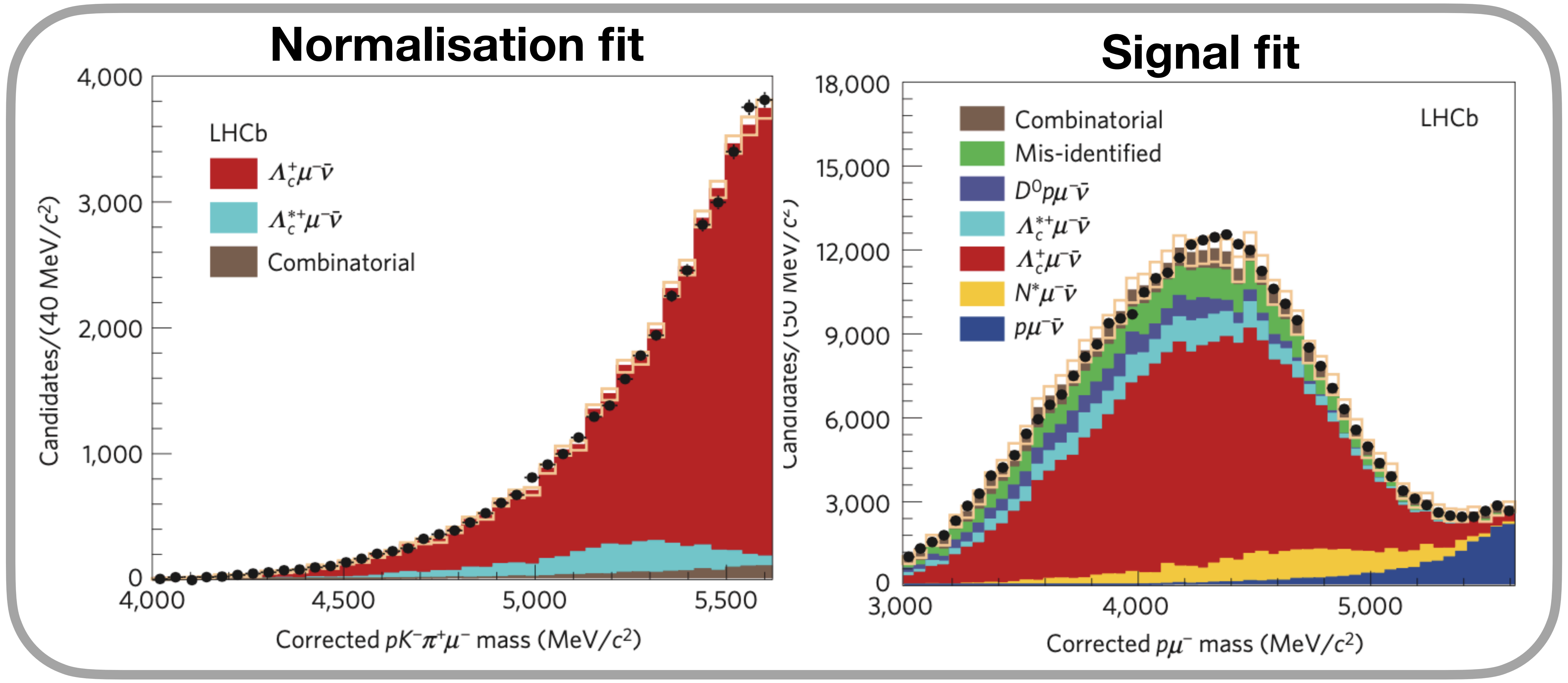

- Extracting $|V_{ub}|$ from the BF ratio:
  → Measured in the high q^2 region.

Target

$$\frac{|V_{ub}|^2}{|V_{cb}|^2}\frac{G(\Lambda_b^0 \to p\mu^-\bar{\nu}_\mu)_{q^2>15\,\text{GeV}^2/c^4}}{G(\Lambda_b^0 \to \Lambda_c^+\mu^-\bar{\nu}_\mu)_{q^2>7\,\text{GeV}^2/c^4}} = \frac{N(\Lambda_b^0 \to p\mu^-\bar{\nu}_\mu)_{q^2>15\,\text{GeV}^2/c^4}}{N(\Lambda_b^0 \to \Lambda_c^+(\to pK^-\pi^+)\mu^-\bar{\nu}_\mu)_{q^2>7\,\text{GeV}^2/c^4}} \times \frac{\epsilon(\Lambda_b^0 \to \Lambda_c^+(\to pK^-\pi^+)\mu^-\bar{\nu}_\mu)_{q^2>7\,\text{GeV}^2/c^4}}{\epsilon(\Lambda_b^0 \to p\mu^-\bar{\nu}_\mu)_{q^2>15\,\text{GeV}}} \times BF(\Lambda_c^+ \to pK^-\pi^+)$$

Yields and efficiencies are estimated in the high q^2 regions (most precise FFs).

Exclusive $|V_{cb}|$ world average [Chin. Phys. C 38, 090001 (2014)].

FFs with LQCD @ high q^2 [Phys.Rev.D 92 (2015)].

BF measured at Belle [Phys. Rev. Lett. 113, 042002 (2014)]

Measuring $|V_{ub}|$ from the $\Lambda_b^0 \to p^+\mu^-\bar{\nu}_\mu$ decay [Nature Physics 11 (2015)]

>> Final analysis result.

$$|V_{ub}| = (3.27 \pm 0.15\,(\text{exp}) \pm 0.16\,(\text{LQCD}) \pm 0.06\,(|V_{cb}|)) \times 10^{-3}$$

P. Owen, Implications workshop 2015

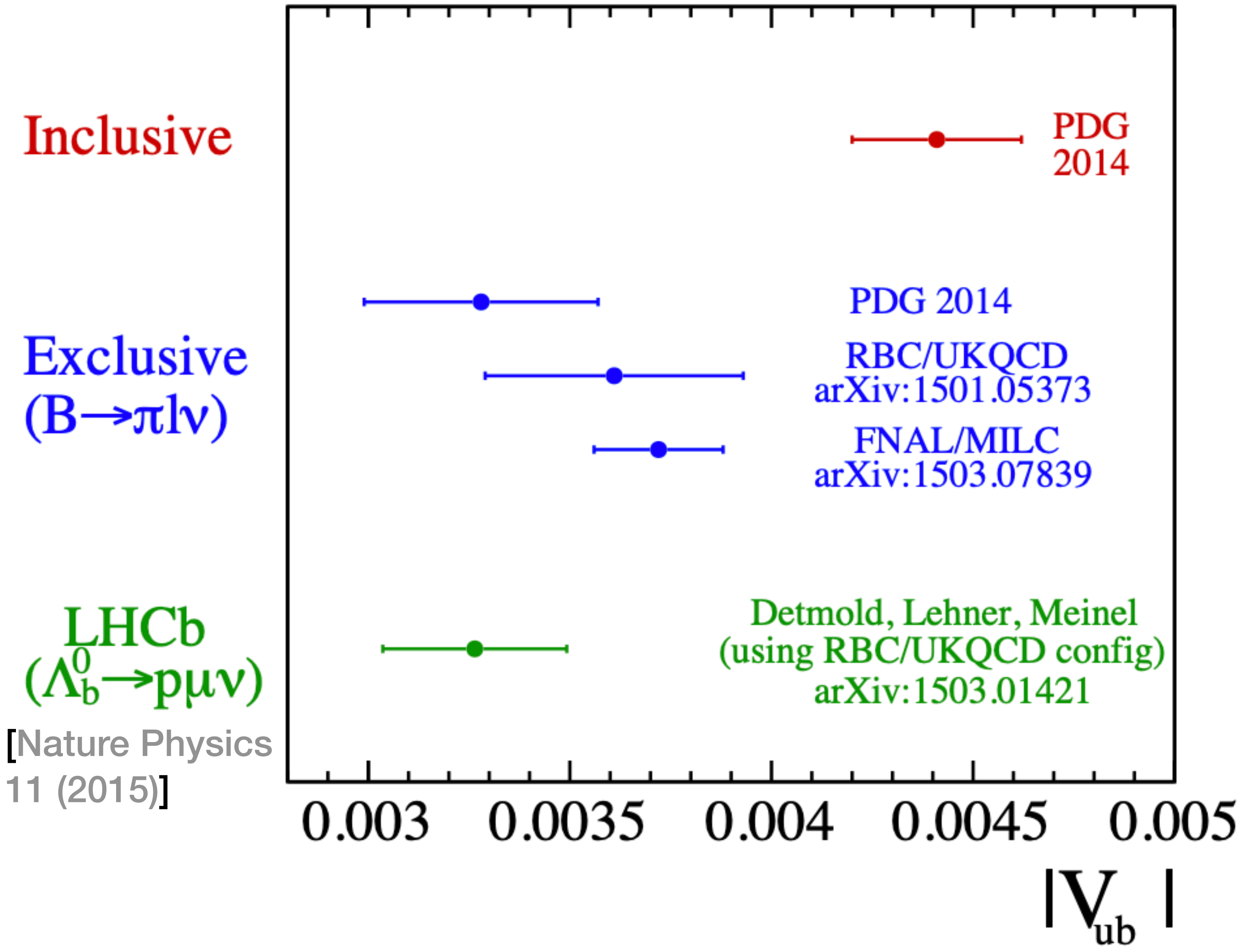

→ agrees with exclusively measured average [arXiv:1412.7515 (2014)].

→ Disagrees ($\sim 3.5\sigma$) with the inclusively measured average [arXiv:1412.7515 (2014)].

Limitations on the $|V_{ub}|$ precision:

→ Approximately equal contributions from experiment and theory.

→ Largest uncertainty comes from LQCD calculations ($\sigma_{FF}/|V_{ub}| \sim 5\,\%$) [Phys.Rev.D 92 (2015)].

→ Largest external uncertainty comes from $\sigma(BF_{\Lambda_c \to pK\pi})/BF_{\Lambda_c \to pK\pi} \sim 5\,\%$ [Phys. Rev. Lett. 113 (2014)].

More recent $BF(\Lambda_c^+ \to pK^-\pi^+)$ average has been used by HFLAV to obtain $|V_{ub}|/|V_{cb}|$ [arXiv:1909.12524, (2021)]

→ will be shown later in this talk.

Measurement of $|V_{ub}|/|V_{cb}|$ from the $B_s^0 \to K^-\mu^+\nu_\mu$ decay [Phys. Rev. Lett. 126 (2021)]

>> First $B_s^0 \to K^-\mu^+\nu_\mu$ observation and $|V_{ub}|$ extraction from B_s^0

- **Dataset:** $2\ \text{fb}^{-1}$ @ $\sqrt{s} = 8$ TeV (Run1, 2012).
- **Signal:** $B_s^0 \to K^-\mu^+\nu_\mu$
- **Normalisation:** $B_s^0 \to D_s^-\mu^+\nu_\mu$ with $D_s^- \to K^-K^+\pi^-$.

Signal fit at low q^2

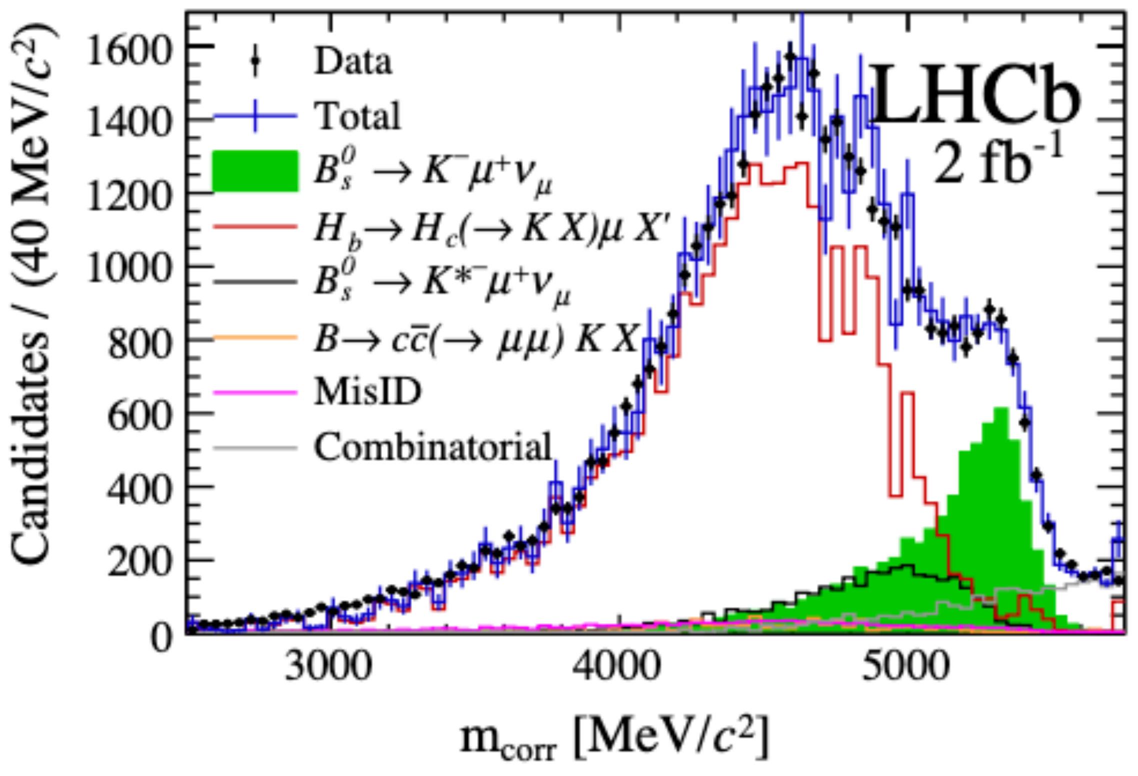

Signal fit at high q^2

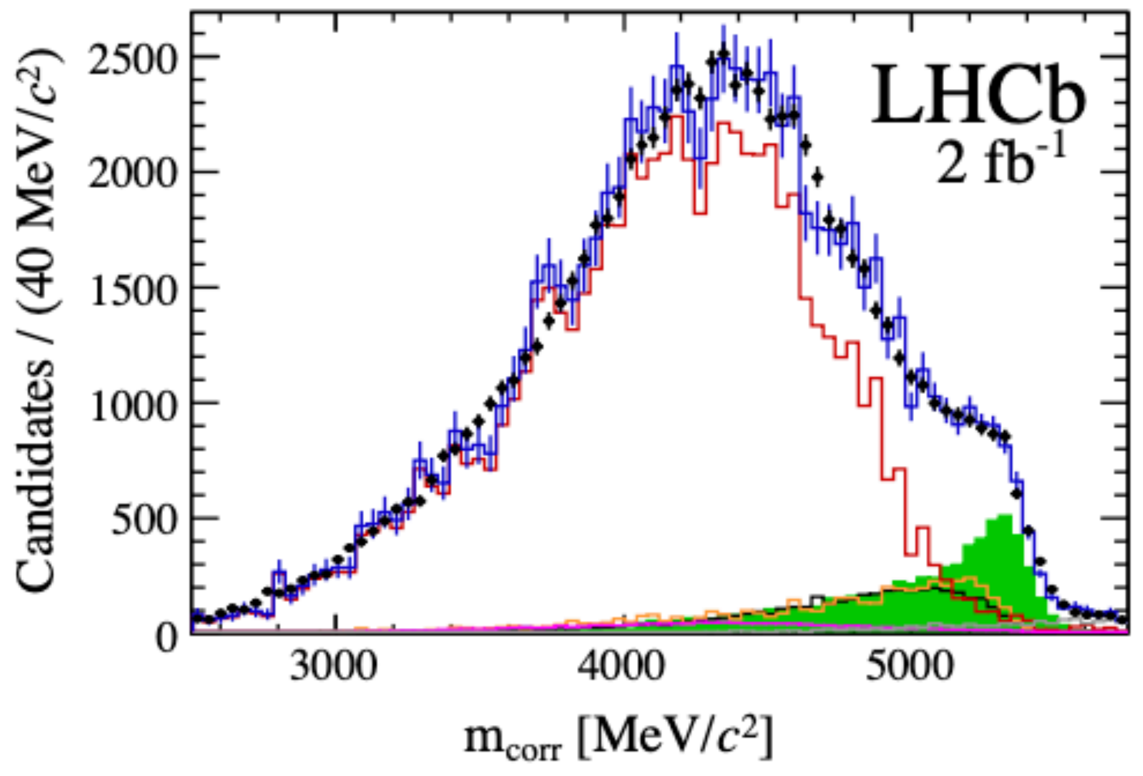

- Extracting $|V_{ub}|/|V_{cb}|$ from the BF ratio:
  $\to$ Measured in two q^2 bins

Target

$$\frac{|V_{ub}|^2}{|V_{cb}|^2}\frac{G(B_s^0 \to K^-\mu^+\nu_\mu)}{G(B_s^0 \to D_s^-\mu^+\nu_\mu)} = \frac{N(B_s^0 \to K^-\mu^+\nu_\mu)}{N(B_s^0 \to D_s^-\mu^+\nu_\mu)} \times \frac{\epsilon(B_s^0 \to D_s^-(\to K^-K^+\pi^-)\mu^+\nu_\mu)}{\epsilon(B_s^0 \to K^-\mu^+\nu_\mu)} \times BF(D_s^- \to K^-K^+\pi^-)$$

FFs for signal :

@ Low q^2 with LCSR [JHEP 2017, 112 (2017)]

@ High q^2 with LQCD [Phys. Rev. D 100, 034501 (2019)]

FFs for normalisation:

@ Full q^2 LQCD [Phys. Rev. D 101, 074513 (2020)]

Yields and efficiencies are estimated in the two q^2 regions.

External BF measurement [Prog. Theor. Exp. Phys. 2020, 083C01 (2020).]

Measurement of $|V_{ub}|/|V_{cb}|$ from the $B_s^0 \to K^- \mu^+ \nu_\mu$ decay [Phys. Rev. Lett. 126 (2021)]

>> Final analysis result.

$q^2 < 7\,\text{GeV}^4/c^2$: $|V_{ub}|/|V_{cb}| = 0.0607 \pm 0.0015\,(\text{stat}) \pm 0.0013\,(\text{syst}) \pm 0.0008\,(D_s) \pm 0.0030\,(\text{FF})$

$q^2 > 7\,\text{GeV}^4/c^2$: $|V_{ub}|/|V_{cb}| = 0.0946 \pm 0.0030\,(\text{stat})^{+0.0024}_{-0.0025}\,(\text{syst}) \pm 0.0013\,(D_s) \pm 0.0068\,(\text{FF})$

→ Tension is **driven by the difference in the FF calculations.**

Limitations on the $|V_{ub}|/|V_{cb}|$ precision:

- **The dominant uncertainty comes from FF calculations:**
  - **Low q2:** $\sigma/(|V_{ub}|/|V_{cb}|) \sim 5\,\%$ [JHEP 2017, 112 (2017)].
  - **High q2:** $\sigma/(|V_{ub}|/|V_{cb}|) \sim 7\,\%$ [Phys. Rev. D 100, 034501 (2019)].

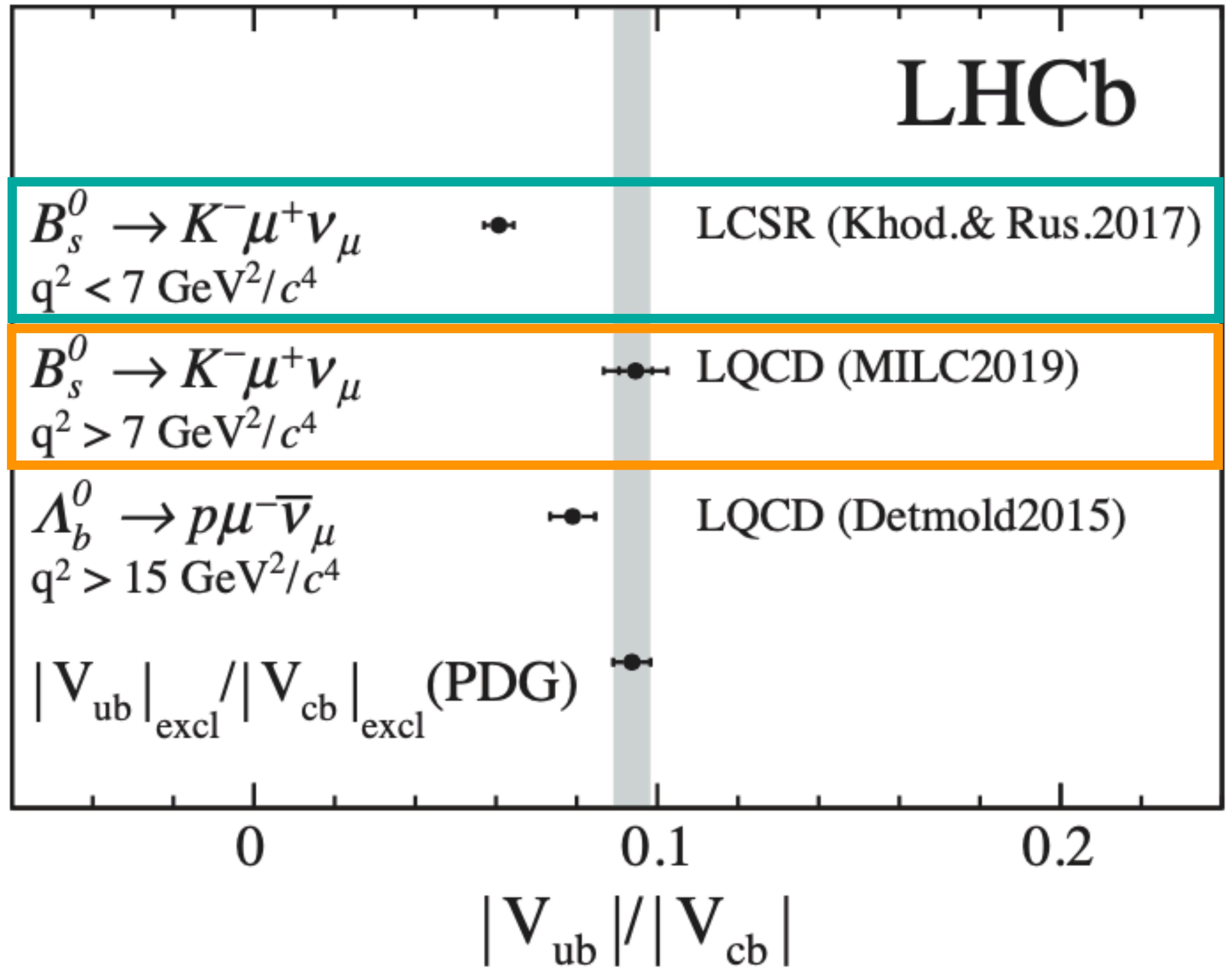

Summary of LHCb $|V_{cb}|$ and $|V_{ub}|$ results

Exclusive & inclusive $|V_{cb}|$

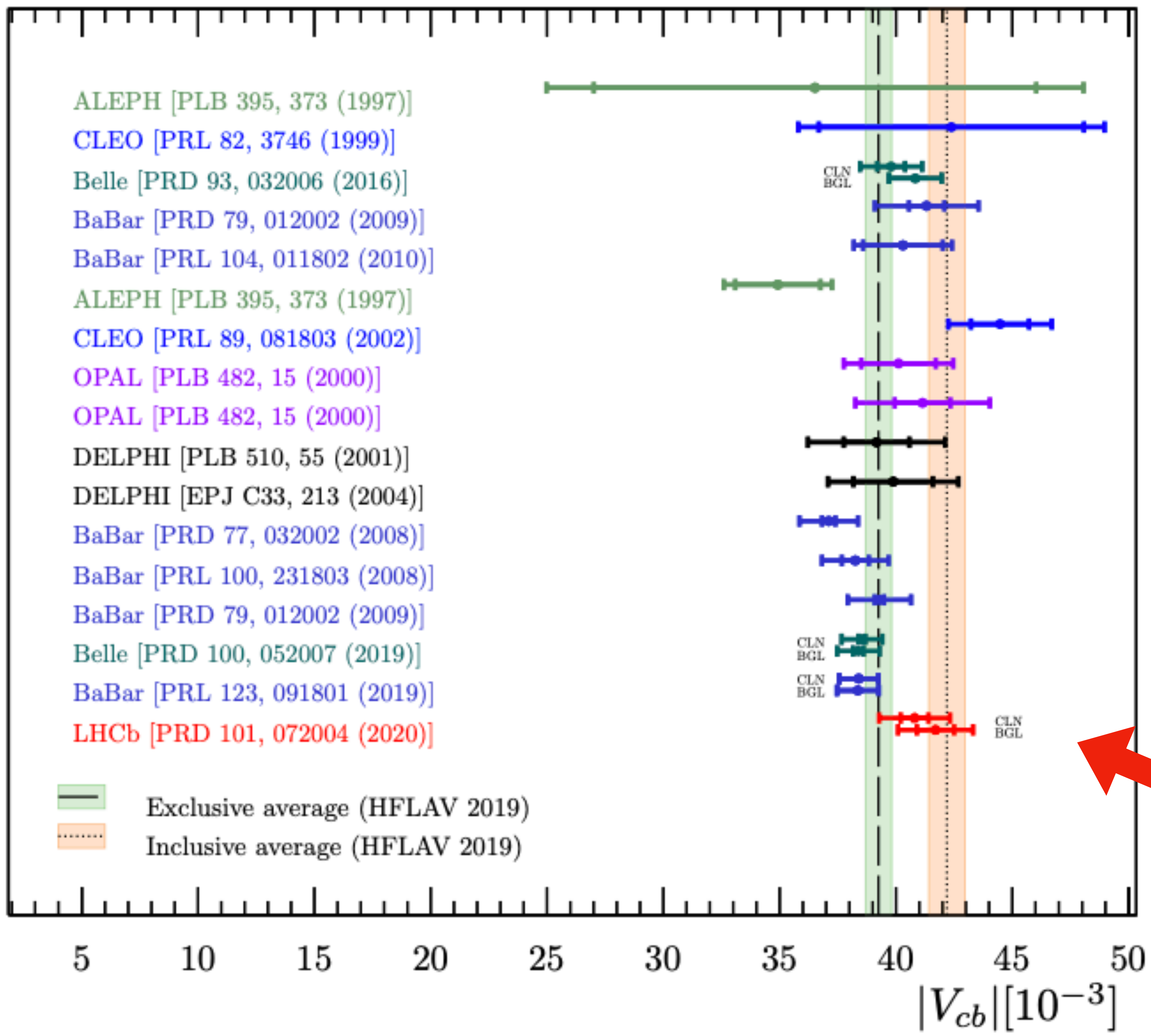

Plot taken from this talk by M. De Cian, FPCP (2021).

[Phys. Rev. Lett. 126 (2021)]
$q^2 > 7\ \text{GeV}^4/c^2$

[Nature Physics 11 (2015)]
updated with recent
$BF(\Lambda_c^+ \to pK^-\pi^+)$
average
[arXiv:1909.12524, (2021)]

[Phys. Rev. Lett. 126 (2021)]
$q^2 < 7\ \text{GeV}^4/c^2$

[Phys. Rev. D 101 (2020)]
updated with latest f_s/f_d
[Phys. Rev. D 104, 032005 (2021)].

Exclusive & inclusive measurements in the $(|V_{cb}|, |V_{ub}|)$ plane

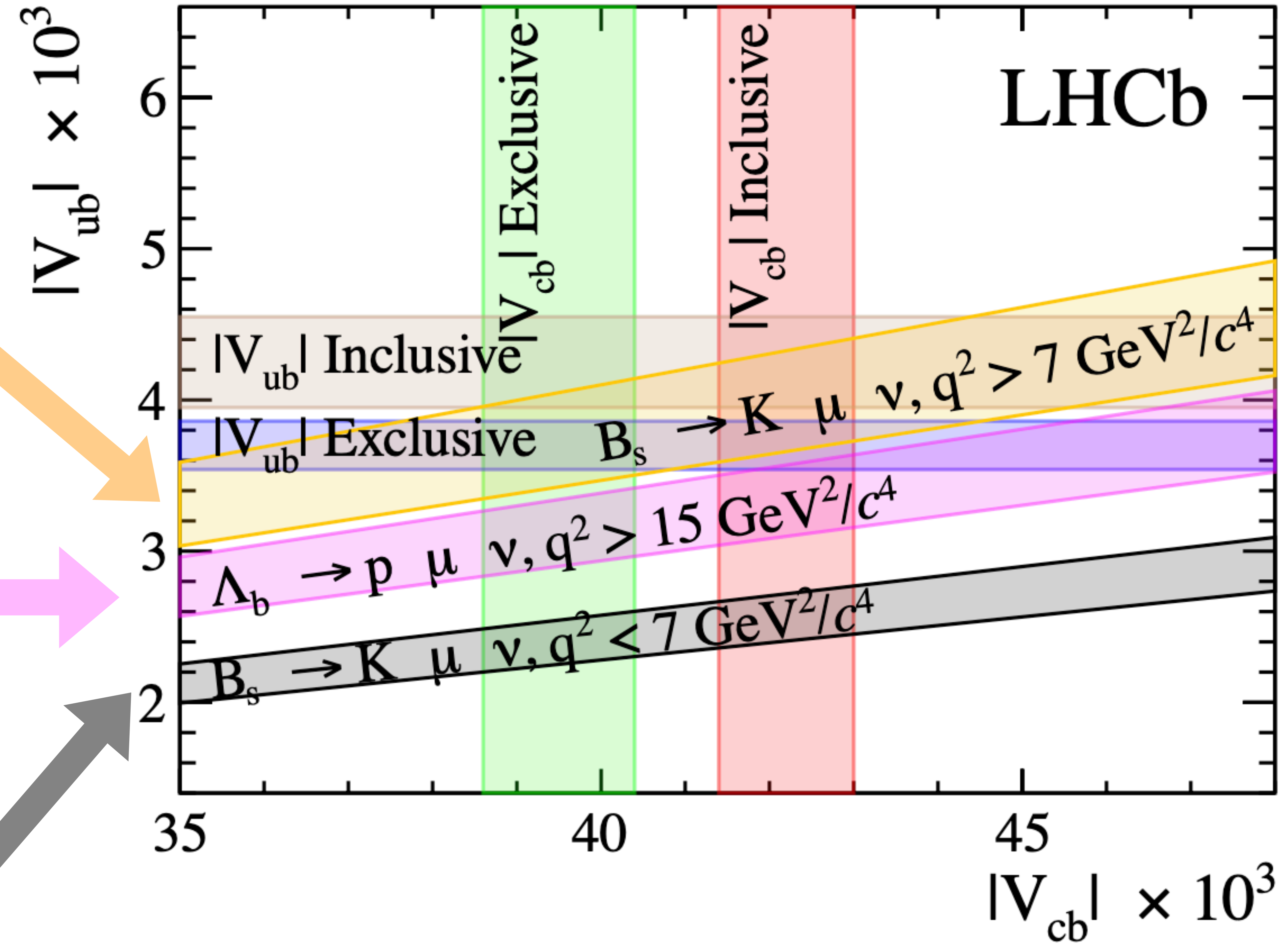

[PRL 126, 081804]

Future measurements at LHCb

1. **Extracting** $|V_{ub}|$ and $B_s^0 \to K^-$ form factor parameters from the $B_s^0 \to K^-\mu^+\nu_\mu$ differential decay rate measured in eight bins of q^2 with Run 2 data.

   → Expecting a ~ 5-6 times higher signal yield wrt. to Run 1 [Phys. Rev. Lett. 126 (2021)].

2. **Extracting** $|V_{ub}|$ and part of the $B^+ \to \rho^0$ BCL FFs from the $B^+ \to \rho^0\mu^+\nu_\mu$ differential decay rate measured in ten bins of q^2 with Run 2 data.

   → Expecting > 50 times higher signal yield wrt. to Belle [Phys. Rev. D 88, 032005 (2013)].

3. **Extracting** $|V_{ub}|/|V_{cb}|$ from $B_c^+ \to D^{(*)0}\mu\nu$ by normalising to $B_c^+ \to J/\psi\mu^+\nu_\mu$ with Run 2 data.

   → First CKM matrix element determined from B_c^+ system.

4. **Extracting** $|V_{cb}|$ from the $\Lambda_b^0 \to \Lambda_c^+\mu^-\bar{\nu}_\mu$ differential decay rate with Run 2 dataset.

   → First determination of $|V_{cb}|$ from a baryonic semileptonic decay.

Conclusion and outlook

- **LHCb has measured $|V_{cb}|$ and $|V_{ub}|$ from new exclusive channels involving Λ_b^0 baryons and B_s^0 mesons.**

  → **Constraining the Unitary Triangle of the CKM matrix**.

  → **Providing complementary information** to **understand the long-standing tension** between the exclusive and inclusive determinations.

- **More LHCb measurements on the way:**

  → **Larger signal samples** (reducing statistical and systematic uncertainties).

  → **Measuring new semileptonic channels** (see slide 18).

  → **Improve $|V_{ub}|$ precision from $B_s^0 \to K^-\mu^+\nu_\mu$ through a differential measurement.**

Thank you for your attention :)

Back-up slides

Back-up slides

Measurement of $|V_{cb}|$ from the $B_s^0 \to D_s^{(*)-}\mu^+\nu_\mu$ decay

Phys. Rev. D 101 (2020)

Selection

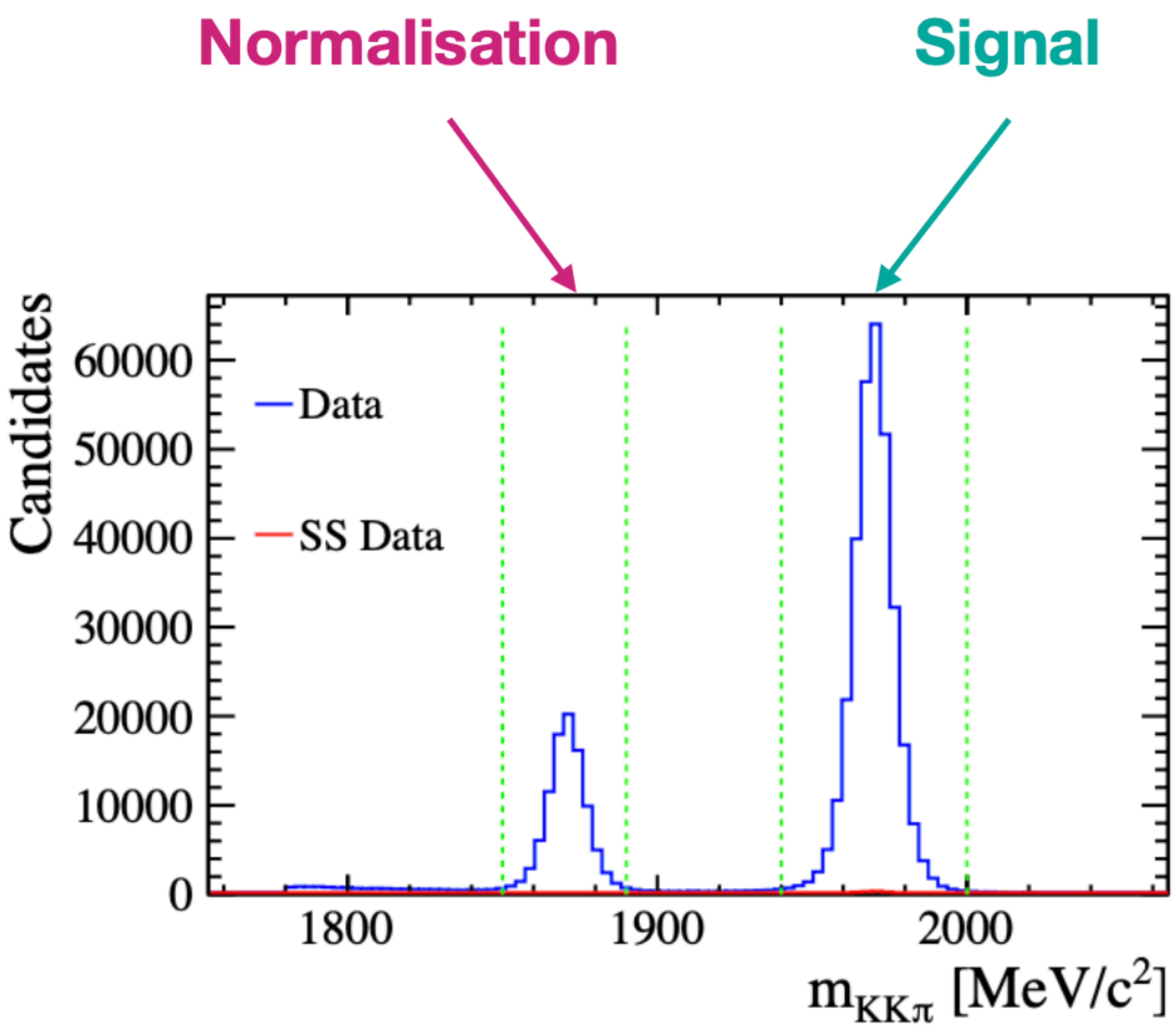
Normalisation
Signal
Candidates
60000
50000
40000
30000
20000
10000
0
Data
SS Data
1800
1900
2000
m_KKπ [MeV/c²]

Normalisation fit

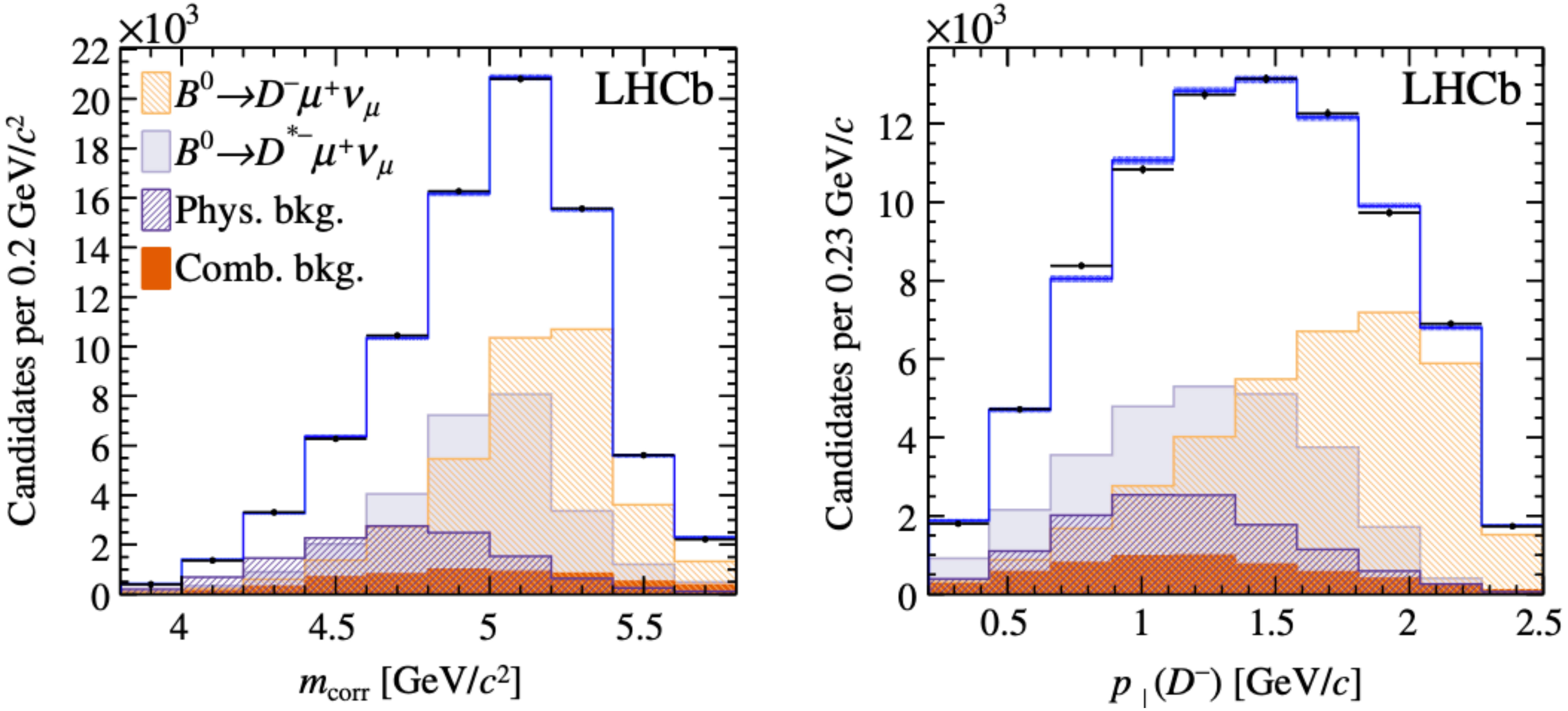

[Phys. Rev. D 101 (2020)]

Background-subtracted distribution of $p_\perp(D_s^-)$

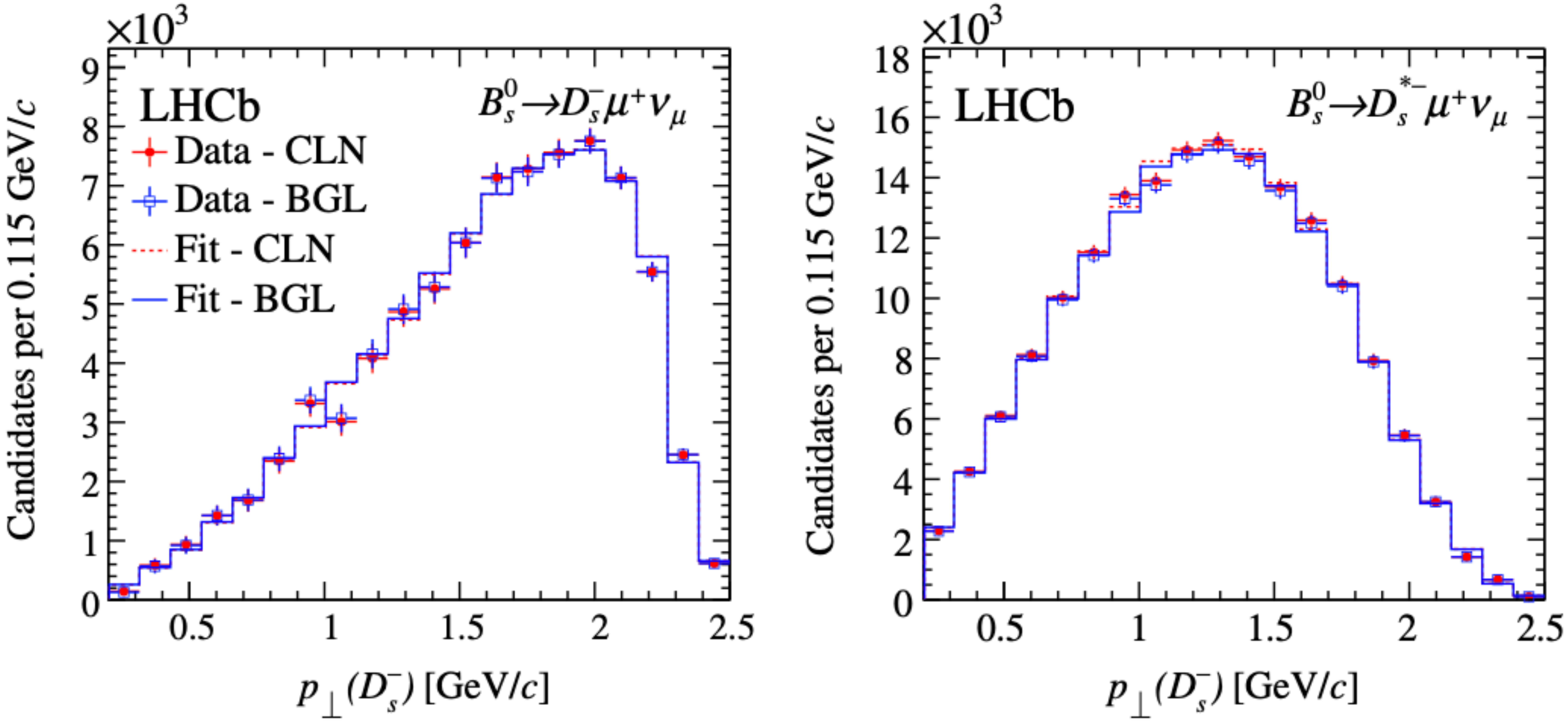

Fit result in the CLN and BGL parameterisation

TABLE V. Fit results in the CLN parametrization. The uncertainty is split into two contributions, statistical (stat) and that due to the external inputs (ext).

Parameter	Value
$\|V_{cb}\|$ $[10^{-3}]$	$41.4 \pm 0.6(\text{stat}) \pm 1.2(\text{ext})$
$\mathcal{G}(0)$	$1.102 \pm 0.034(\text{stat}) \pm 0.004(\text{ext})$
$\rho^2(D_s^-)$	$1.27 \pm 0.05(\text{stat}) \pm 0.00(\text{ext})$
$\rho^2(D_s^{*-})$	$1.23 \pm 0.17(\text{stat}) \pm 0.01(\text{ext})$
$R_1(1)$	$1.34 \pm 0.25(\text{stat}) \pm 0.02(\text{ext})$
$R_2(1)$	$0.83 \pm 0.16(\text{stat}) \pm 0.01(\text{ext})$

TABLE VI. Fit results in the BGL parametrization. The uncertainty is split into two contributions, statistical (stat) and that due to the uncertainty on the external inputs (ext).

Parameter	Value
$\|V_{cb}\|$ $[10^{-3}]$	$42.3 \pm 0.8(\text{stat}) \pm 1.2(\text{ext})$
$\mathcal{G}(0)$	$1.097 \pm 0.034(\text{stat}) \pm 0.001(\text{ext})$
d_1	$-0.017 \pm 0.007(\text{stat}) \pm 0.001(\text{ext})$
d_2	$-0.26 \pm 0.05(\text{stat}) \pm 0.00(\text{ext})$
b_1	$-0.06 \pm 0.07(\text{stat}) \pm 0.01(\text{ext})$
a_0	$0.037 \pm 0.009(\text{stat}) \pm 0.001(\text{ext})$
a_1	$0.28 \pm 0.26(\text{stat}) \pm 0.08(\text{ext})$
c_1	$0.0031 \pm 0.0022(\text{stat}) \pm 0.0006(\text{ext})$

[Phys. Rev. D 101 (2020)]

Summary of the fit parameter uncertainties

TABLE VII. Summary of the uncertainties affecting the measured parameters. The upper section reports the systematic uncertainties due to the external inputs (ext), the middle section those due to the experimental methods (syst), and the lower section the statistical uncertainties (stat). For the first source of uncertainty the multiplication by τ holds only for the $|V_{cb}|$ fits.

	Uncertainty															
	CLN parametrization						BGL parametrization									
Source	$\lvert V_{cb}\rvert$ $[10^{-3}]$	$\rho^2(D_s^-)$ $[10^{-1}]$	$\mathcal{G}(0)$ $[10^{-2}]$	$\rho^2(D_s^{*-})$ $[10^{-1}]$	$R_1(1)$ $[10^{-1}]$	$R_2(1)$ $[10^{-1}]$	$\lvert V_{cb}\rvert$ $[10^{-3}]$	d_1 $[10^{-2}]$	d_2 $[10^{-1}]$	$\mathcal{G}(0)$ $[10^{-2}]$	b_1 $[10^{-1}]$	c_1 $[10^{-3}]$	a_0 $[10^{-2}]$	a_1 $[10^{-1}]$	$\mathcal{R}$ $[10^{-1}]$	$\mathcal{R}^*$ $[10^{-1}]$
$f_s/f_d \times \mathcal{B}(D_s^- \to K^+K^-\pi^-)(\times\tau)$	0.8	0.0	0.0	0.0	0.0	0.0	0.8	0.0	0.0	0.0	0.0	0.0	0.0	0.1	0.4	0.4
$\mathcal{B}(D^- \to K^-K^+\pi^-)$	0.5	0.0	0.0	0.0	0.0	0.0	0.5	0.0	0.0	0.0	0.0	0.0	0.0	0.1	0.3	0.3
$\mathcal{B}(D^{*-} \to D^-X)$	0.2	0.0	0.1	0.0	0.1	0.0	0.1	0.0	0.0	0.1	0.0	0.2	0.0	0.3	...	0.2
$\mathcal{B}(B^0 \to D^-\mu^+\nu_\mu)$	0.4	0.0	0.3	0.1	0.2	0.1	0.5	0.1	0.0	0.1	0.1	0.4	0.1	0.7	...	...
$\mathcal{B}(B^0 \to D^{*-}\mu^+\nu_\mu)$	0.3	0.0	0.2	0.1	0.1	0.1	0.2	0.0	0.0	0.1	0.1	0.3	0.1	0.4	...	...
$m(B_s^0)$, $m(D^{(*)-})$	0.0	0.0	0.0	0.0	0.0	0.0	0.0	0.0	0.0	0.0	0.0	0.0	0.0	0.1	...	...
η_{EW}	0.2	0.0	0.0	0.0	0.0	0.0	0.2	0.0	0.0	0.0	0.0	0.0	0.0	0.1	...	...
$h_{A_1}(1)$	0.3	0.0	0.2	0.1	0.1	0.1	0.3	0.0	0.0	0.1	0.1	0.3	0.1	0.5	...	...
External inputs (ext)	1.2	0.0	0.4	0.1	0.2	0.1	1.2	0.1	0.0	0.1	0.1	0.6	0.1	0.8	0.5	0.5
$D_{(s)}^- \to K^+K^-\pi^-$ model	0.8	0.0	0.0	0.0	0.0	0.0	0.8	0.0	0.0	0.0	0.0	0.0	0.0	0.0	0.5	0.4
Background	0.4	0.3	2.2	0.5	0.9	0.7	0.1	0.5	0.2	2.3	0.7	2.0	0.5	2.0	0.4	0.6
Fit bias	0.0	0.0	0.0	0.0	0.0	0.0	0.2	0.0	0.0	0.0	0.2	0.4	0.2	0.4	0.0	0.0
Corrections to simulation	0.0	0.0	0.5	0.0	0.1	0.0	0.0	0.1	0.0	0.1	0.0	0.0	0.0	0.1	0.0	0.0
Form-factor parametrization	...	...	...	...	...	...	...	...	...	...	...	...	...	...	0.0	0.1
Experimental (syst)	0.9	0.3	2.2	0.5	0.9	0.7	0.9	0.5	0.2	2.3	0.7	2.1	0.5	2.0	0.6	0.7
Statistical (stat)	0.6	0.5	3.4	1.7	2.5	1.6	0.8	0.7	0.5	3.4	0.7	2.2	0.9	2.6	0.5	0.5

[Phys. Rev. D 101 (2020)]

$|V_{cb}|$ extraction and relative uncertainties

$$|V_{cb}|_{\mathrm{CLN}} = (41.4 \pm 0.6\,(\textbf{stat}) \pm 0.9\,(\textbf{syst}) \pm 1.2\,(\textbf{ext})) \times 10^{-3} = (41.4 \pm 1.6\,(\textbf{tot})) \times 10^{-3}$$

(~1.4%) (~2.2%) (~2.9%) (~3.9%)

$$|V_{cb}|_{\mathrm{BGL}} = (42.3 \pm 0.8\,(\textbf{stat}) \pm 0.9\,(\textbf{syst}) \pm 1.2\,(\textbf{ext})) \times 10^{-3} = (42.3 \pm 1.7\,(\textbf{tot})) \times 10^{-3}$$

(~1.9%) (~2.1%) (~2.8%) (~4.0%)

Back-up slides

Measurement of the shape of the $B_s^0 \to D_s^{(*)-}\mu^+\nu_\mu$ differential decay rate

J. High Energ. Phys. 144 (2020)

Fully reconstructed D_s^* meson

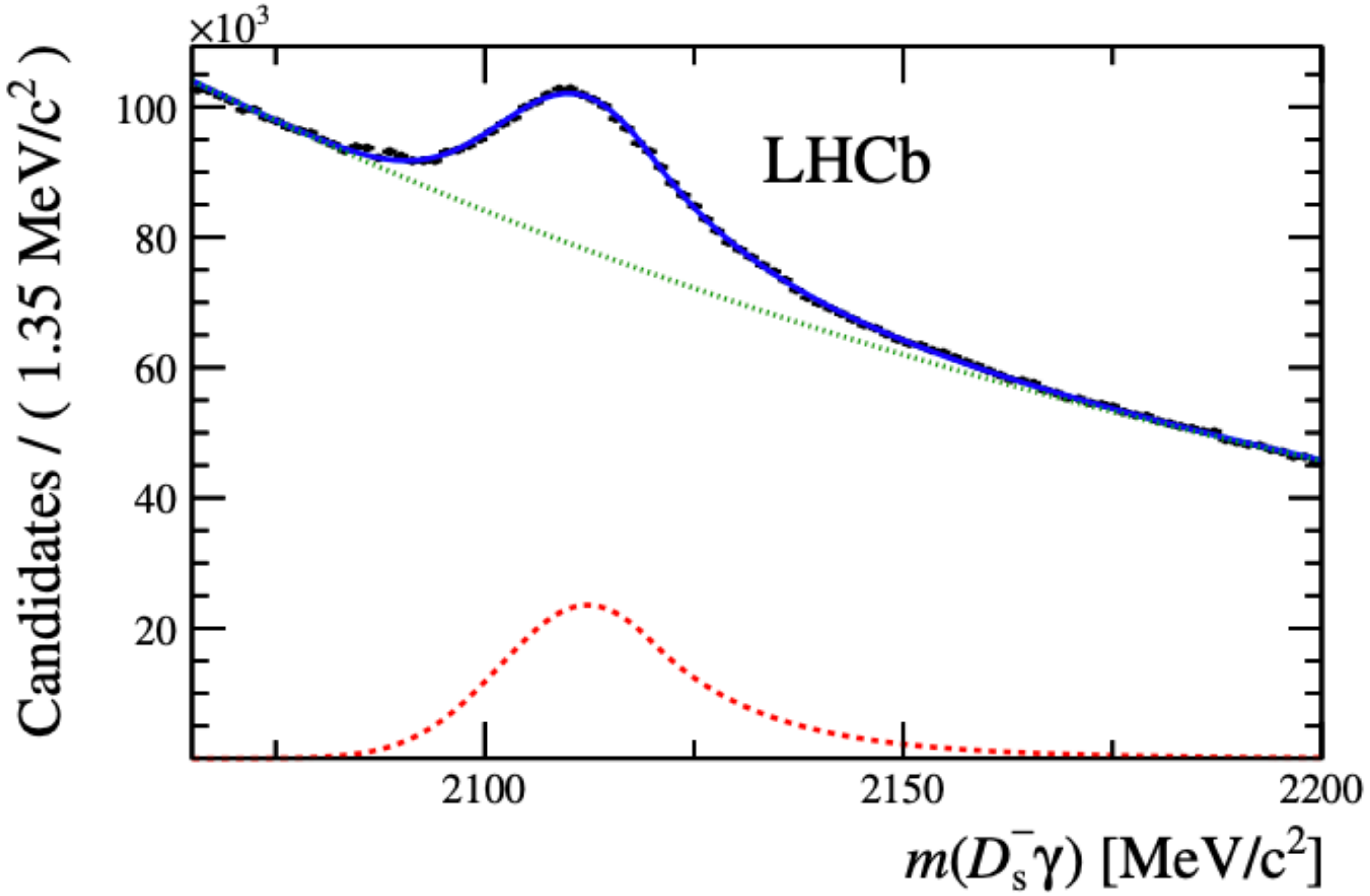

Figure 2. Distribution of the reconstructed $D_s^-\gamma$ mass, $m(D_s^-\gamma)$, with the fit overlaid. The fit is performed constraining the D_s^- mass to the world-average value [16]. The signal and background components are shown separately with dashed red and dotted green lines, respectively.

[J. High Energ. Phys. 144 (2020)]

Signal fits in bins of w

bin	1	2	3	4	5	6	7
w	1.1087	1.1688	1.2212	1.2717	1.3226	1.3814	1.4667

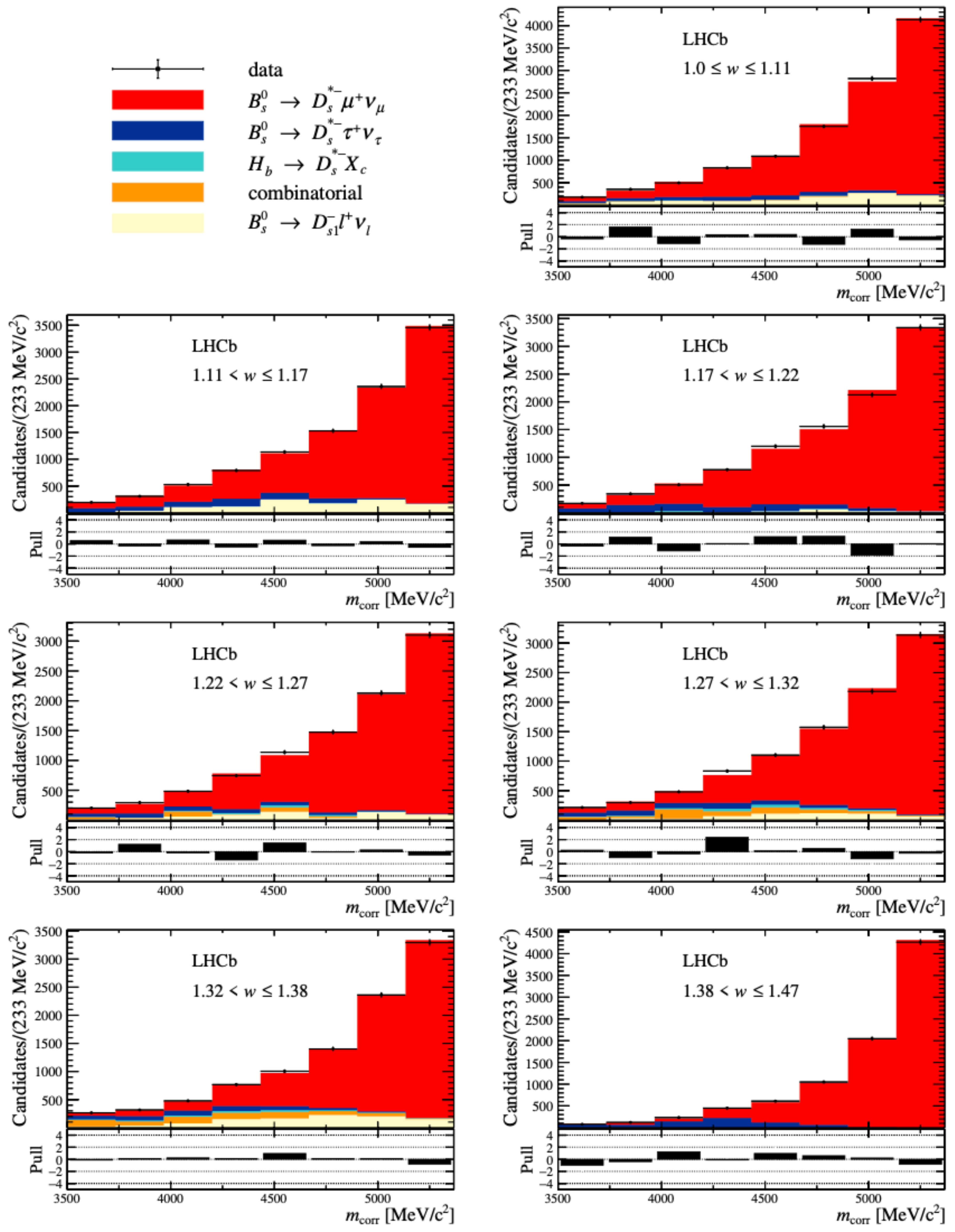

Figure 3. Distribution of the corrected mass, m_{corr}, for the seven bins of w, overlaid with the fit results. The $B_s^0 \to D_{s1}(2460)^-\tau^+\nu_\tau$ and the $B_s^0 \to D_{s1}(2460)^-\mu^+\nu_\mu$ components are combined in $B_s^0 \to D_{s1}(2460)^-\ell^+\nu_\ell$. Below each plot, differences between the data and fit are shown, normalised by the uncertainty in the data.

[J. High Energ. Phys. 144 (2020)]

BGL and CLN FF results and uncertainties

CLN result:

$$\rho^2 = 1.16 \pm 0.05\,(\text{stat}) \pm 0.07\,(\text{syst}),$$

BGL result:

$$a_1^f = -0.005 \pm 0.034\,(\text{stat}) \pm 0.046\,(\text{syst}),$$
$$a_2^f = 1.00\,^{+0.00}_{-0.19}\,(\text{stat})\,^{+0.00}_{-0.38}\,(\text{syst}).$$

Source	$\sigma(\rho^2)$	$\sigma(a_1^f)$	$\sigma(a_2^f)$
Simulation sample size	0.053	0.036	$^{+0.00}_{-0.35}$
Sample sizes for efficiencies and corrections	0.020	0.016	$^{+0.00}_{-0.15}$
SVD unfolding regularisation	0.008	0.004	–
Radiative corrections	0.004	–	–
Simulation FF parametrisation	0.007	0.005	–
Kinematic corrections	0.024	0.012	–
Hardware-trigger efficiency	0.001	0.008	–
Software-trigger efficiency	0.004	0.002	–
D_s^- selection efficiency	–	0.008	–
Photon background subtraction	0.002	0.015	–
External parameters in fit	0.024	0.002	$^{+0.00}_{-0.04}$
Total systematic uncertainty	0.068	0.046	$^{+0.00}_{-0.38}$
Statistical uncertainty	0.052	0.034	$^{+0.00}_{-0.19}$

Table 4. Summary of the systematic and statistical uncertainties on the parameters ρ^2, a_1^f and a_2^f from the unfolded CLN and BGL fits. The total systematic uncertainty is obtained by adding the individual components in quadrature.

[J. High Energ. Phys. 144 (2020)]

Comparing with previous LHCb measurements

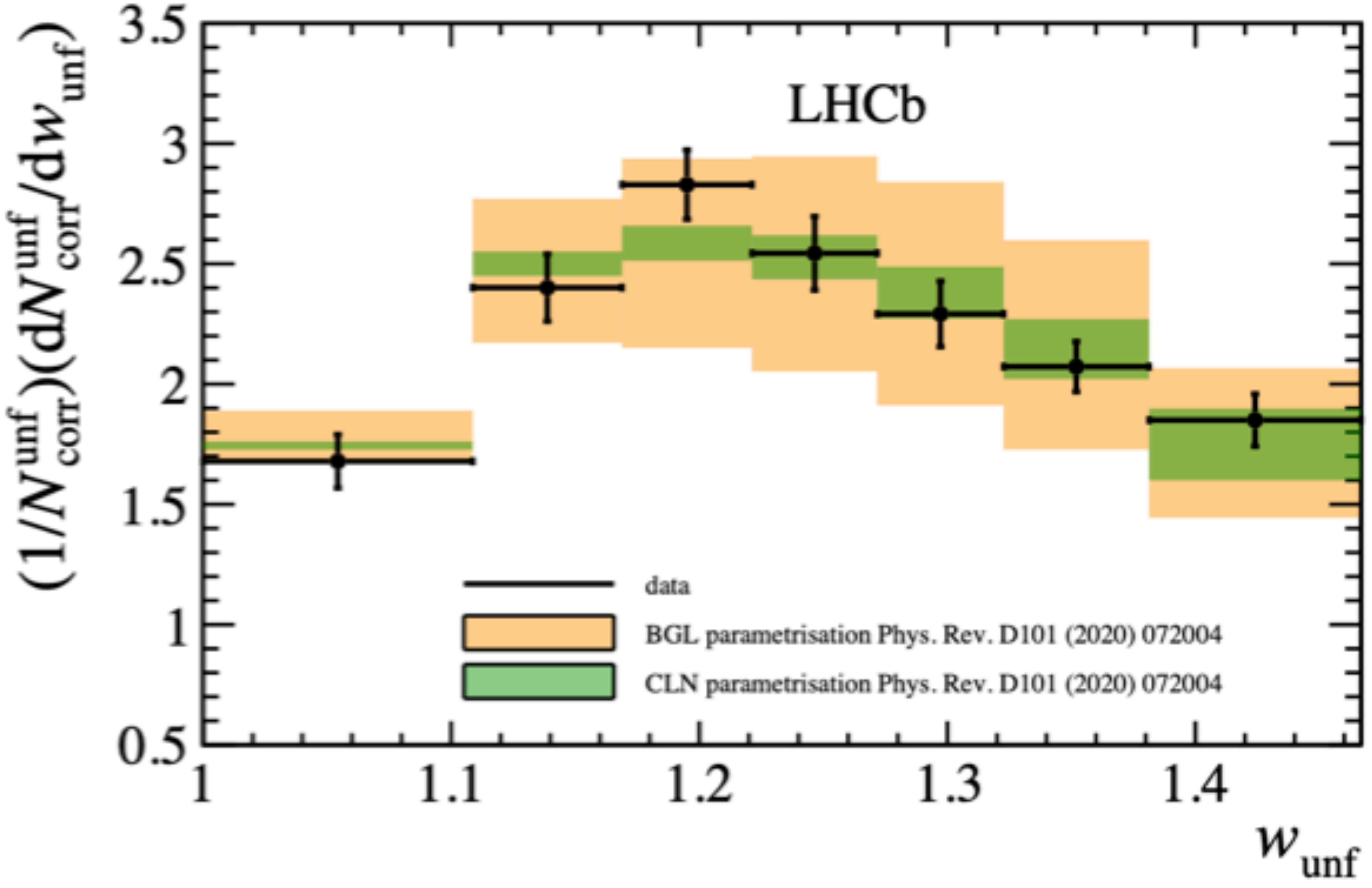

→ Agrees with spectra inferred from Phys. Rev. D 101 (2020).

Back-up slides

Measurement of $|V_{ub}|$ from the $\Lambda_b^0 \to p^+\mu^-\bar{\nu}_\mu$ decay

Nature Physics 11 (2015)

[Nature Physics 11 (2015)]

Mass fits

- Yields are extracted from fits to the $m_{\text{corr}}(\Lambda_b^0)$ distribution:

$$N_{\text{sig}}(q^2 > 15\,\text{GeV}^2/c^4) = 17687 \pm 733 \;(\sim 4\,\%)$$

$\rightarrow$ First observation of $\Lambda_b^0 \rightarrow p\mu^-\bar{\nu}_\mu$.

$$N_{\text{norm}}(q^2 > 7\,\text{GeV}^2/c^4) = 34255 \pm 571 \;(\sim 2\,\%)$$

Unphysical q^2 solutions are removed
$\rightarrow$ no candidates above $m(\Lambda_b^0)$.

Signal channel fit

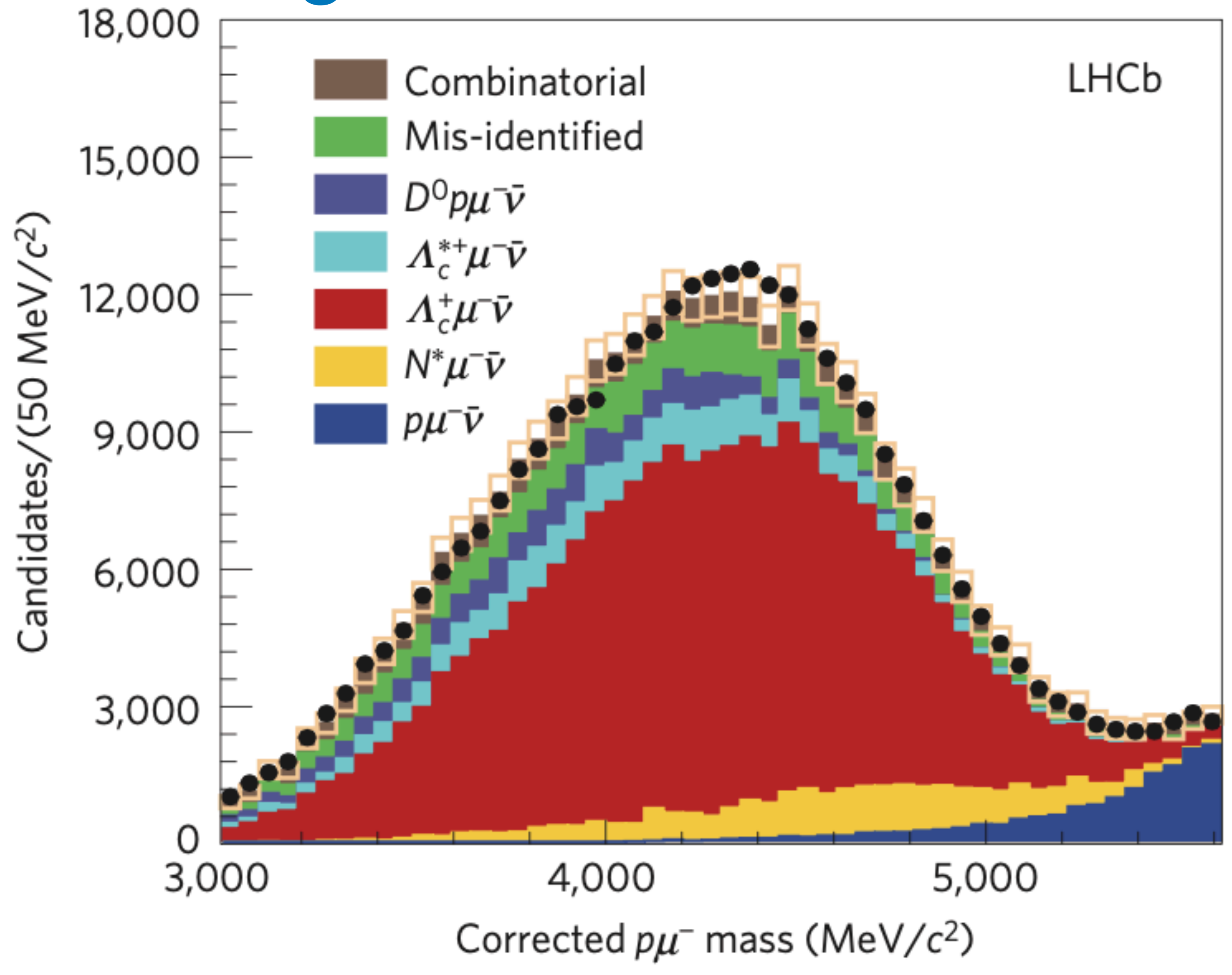

Normalisation channel fit

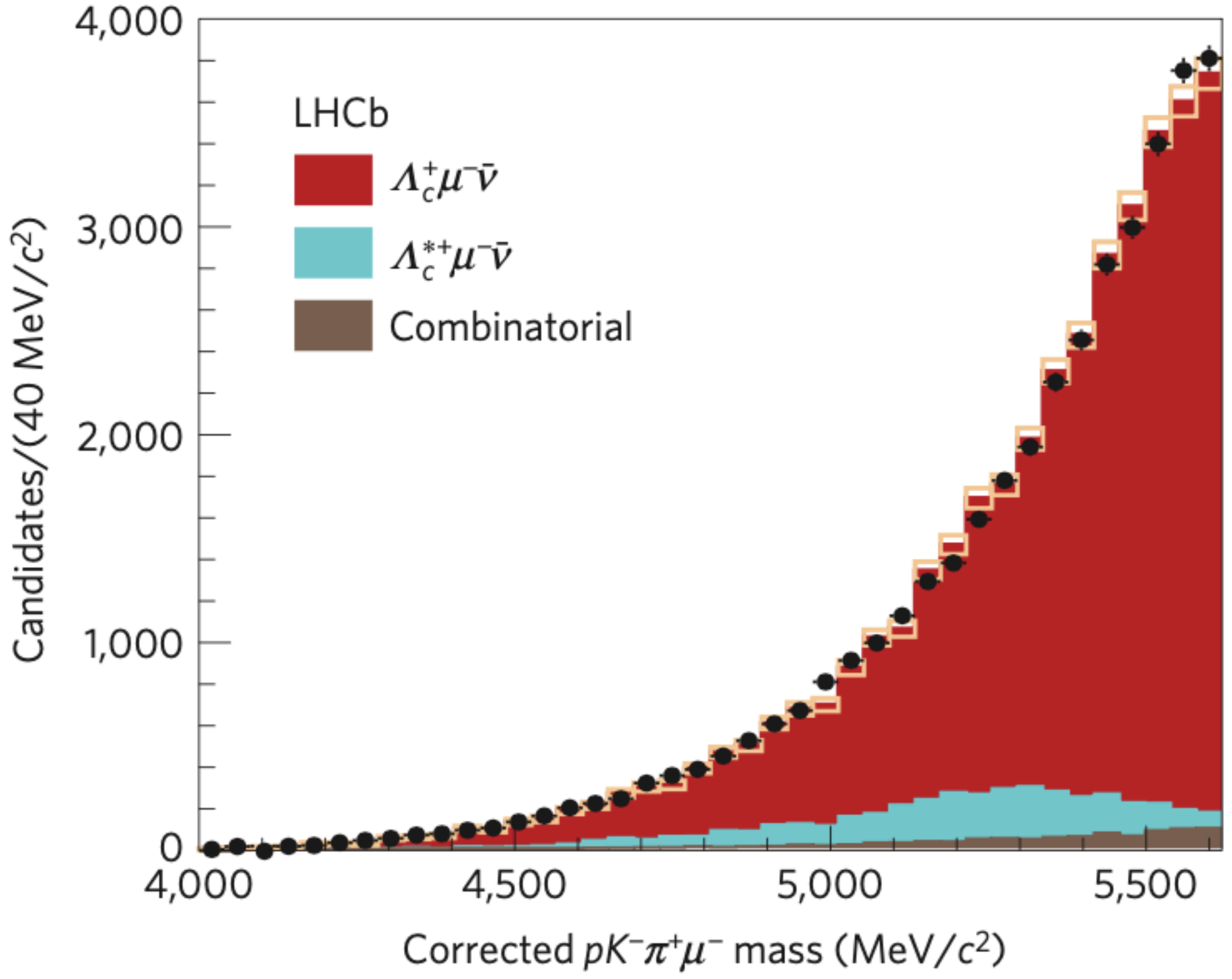

Systematic uncertainties

Table 1 | Summary of systematic uncertainties.

Source	Relative uncertainty (%)
$\mathcal{B}(\Lambda_c^+ \to pK^+\pi^-)$	$^{+4.7}_{-5.3}$
Trigger	3.2
Tracking	3.0
Λ_c^+ selection efficiency	3.0
$\Lambda_b^0 \to N^*\mu^-\overline{\nu}_\mu$ shapes	2.3
Λ_b^0 lifetime	1.5
Isolation	1.4
Form factor	1.0
Λ_b^0 kinematics	0.5
q^2 migration	0.4
PID	0.2
Total	$^{+7.8}_{-8.2}$

The table shows the relative systematic uncertainty on the ratio of the $\Lambda_b^0 \to p\mu^-\overline{\nu}_\mu$ and $\Lambda_b^0 \to \Lambda_c^+\mu^-\overline{\nu}_\mu$ branching fractions broken into its individual contributions. The total is obtained by adding them in quadrature. Uncertainties on the background levels are not listed here as they are incorporated into the fits.

Right-handed current

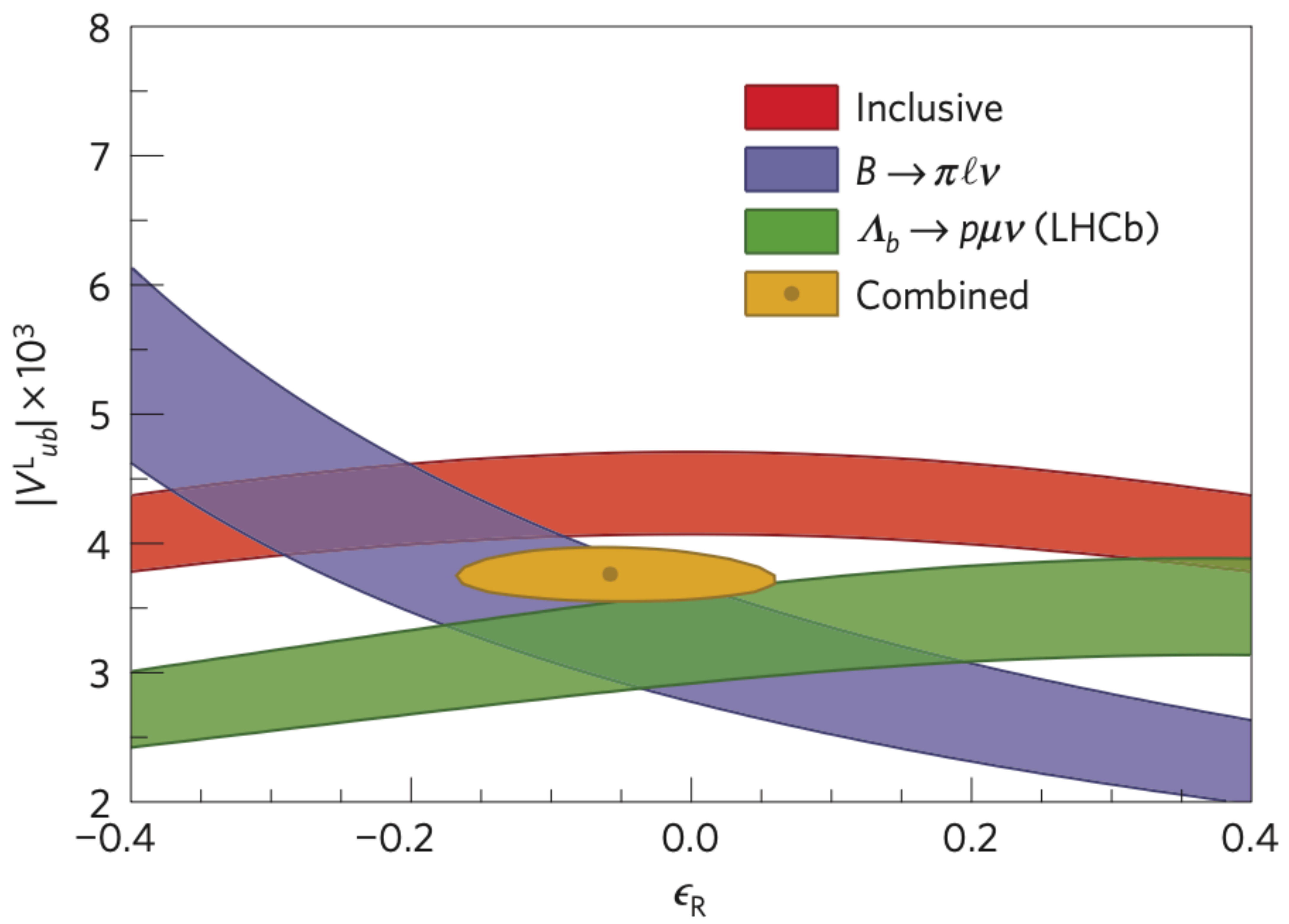

Figure 4 | Experimental constraints on the left-handed coupling, $|V^L_{ub}|$ and the fractional right-handed coupling, ϵ_R. Whereas the overlap of the 68% confidence level bands for the inclusive[14] and exclusive[7] world averages of past measurements suggested a right-handed coupling of significant magnitude, the inclusion of the LHCb $|V_{ub}|$ measurement does not support this.

[Nature Physics 11 (2015)]

$|V_{ub}|$ extraction and relative uncertainties

$$|V_{ub}| = (3.27 \pm 0.15\,(\textbf{exp}) \pm 0.16\,(\textbf{LQCD}) \pm 0.06\,(|V_{cb}|)) \times 10^{-3} = (3.27 \pm 0.23\,(\textbf{tot})) \times 10^{-3}$$

(~4.6%) (~5.0%) (~1.8%) (~7.0%)

Back-up slides

Measurement of $|V_{ub}|/|V_{cb}|$ from the $B_s^0 \to K^- \mu^+ \nu_\mu$ decay

Phys. Rev. Lett. 126 (2021)

Mass fits

- **Yields** are determined from fits to $m_{\text{corr}}(B_s^0)$.

Signal fit → two q^2 bins.

$$N_{\text{sig}}(q^2 < 7\,\text{GeV}^4/c^2) = 6922 \pm 285 \;(\sim 4\,\%)$$

$$N_{\text{sig}}(q^2 > 7\,\text{GeV}^4/c^2) = 6399 \pm 370 \;(\sim 6\,\%)$$

→ first observation of $B_s^0 \to K^- \mu^+ \nu_\mu$.

Norm fit → full q^2 region.

$$N_{\text{norm}} = 201450 \pm 5200 \;(\sim 3\,\%)$$

Signal fit at low q^2

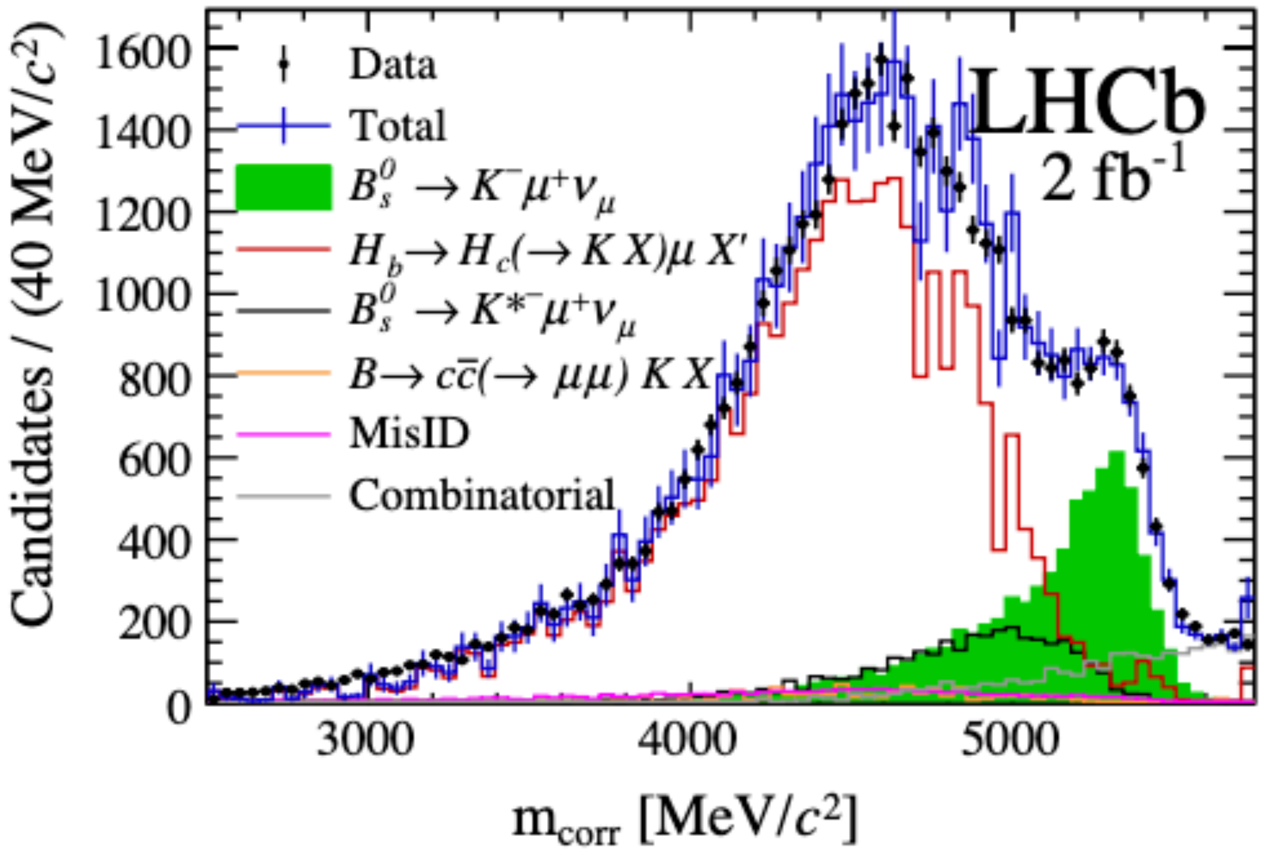

Signal fit at high q^2

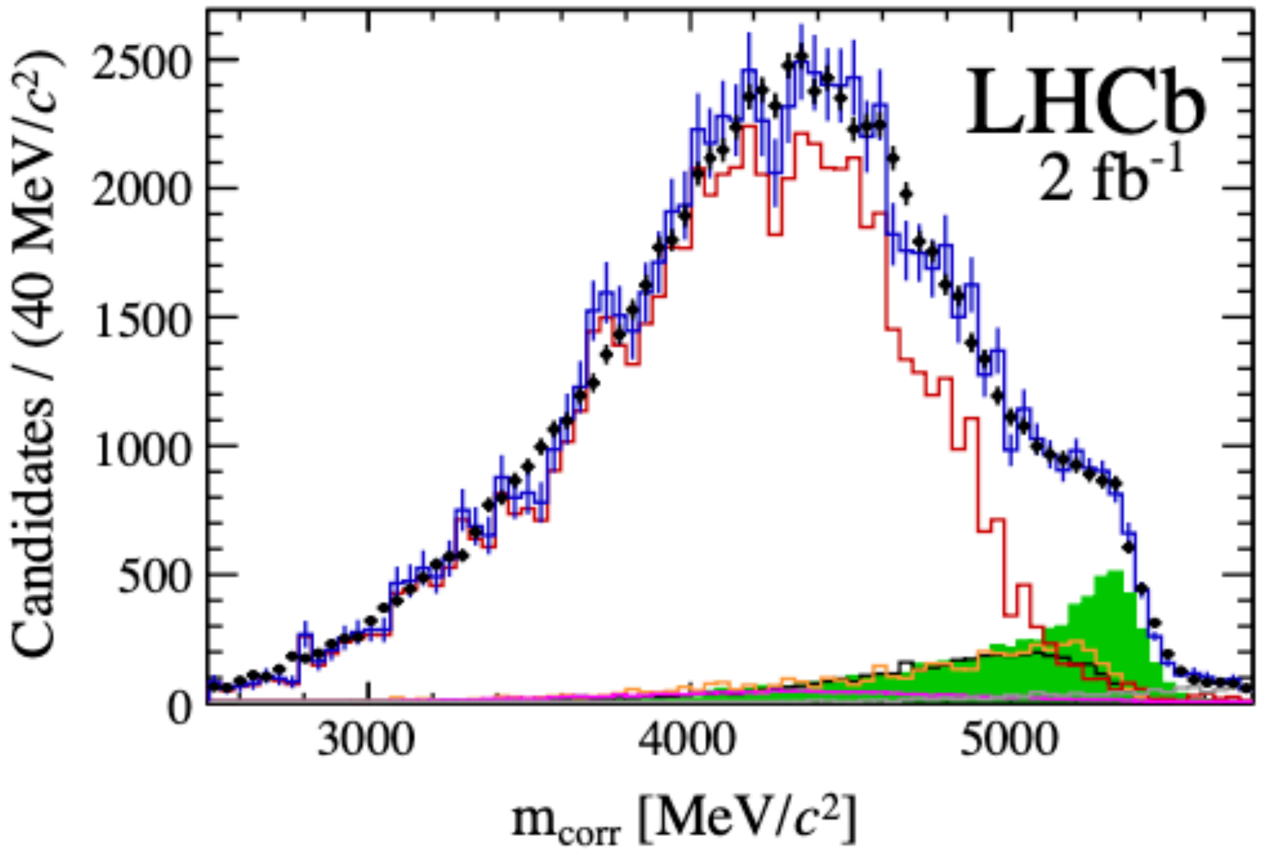

Normalisation fit in full q^2 region

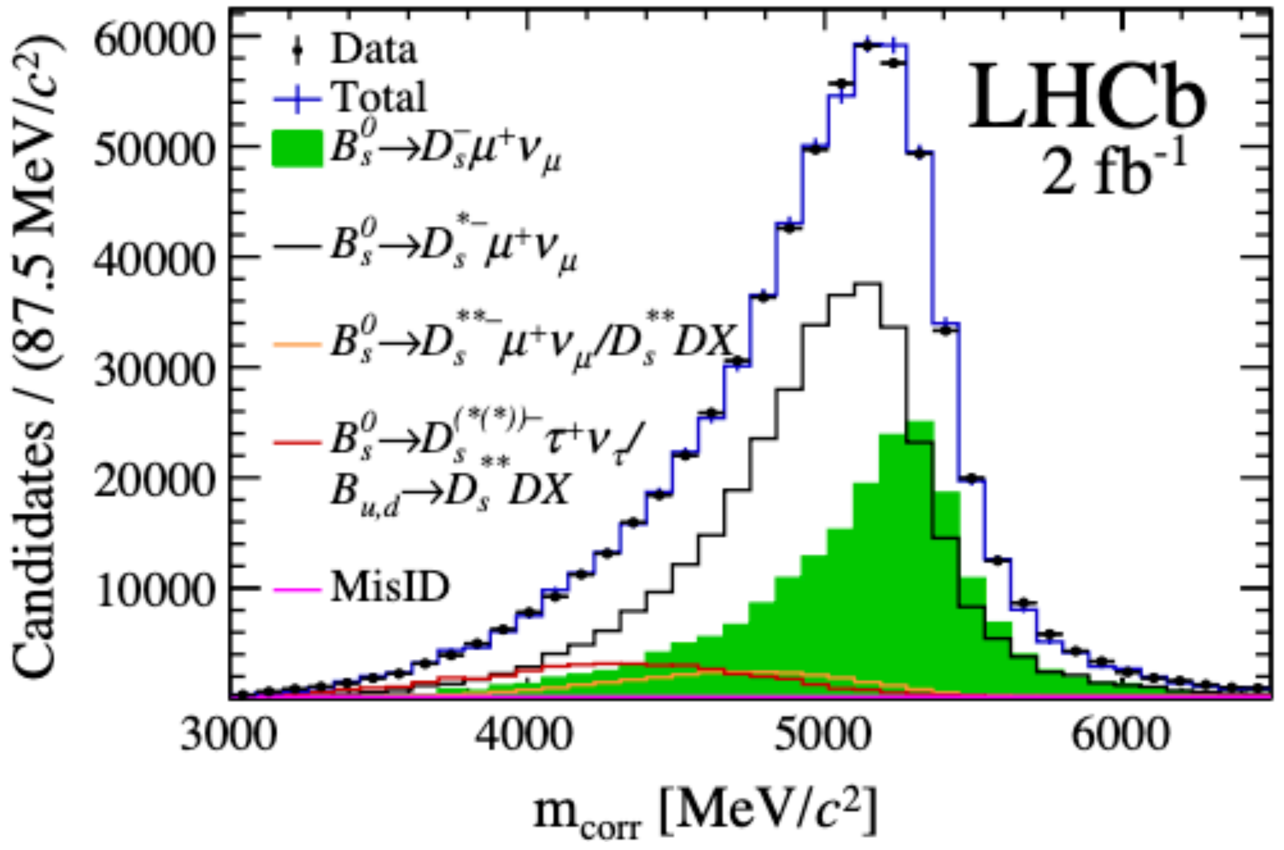

Systematic uncertainties

TABLE I. Relative systematic uncertainties on the ratio $\mathcal{B}(B_s^0 \to K^- \mu^+ \nu_\mu)/\mathcal{B}(B_s^0 \to D_s^- \mu^+ \nu_\mu)$, in percent.

Uncertainty	All q^2	Low q^2	High q^2
Tracking	2.0	2.0	2.0
Trigger	1.4	1.2	1.6
Particle identification	1.0	1.0	1.0
$\sigma(m_{corr})$	0.5	0.5	0.5
Isolation	0.2	0.2	0.2
Charged BDT	0.6	0.6	0.6
Neutral BDT	1.1	1.1	1.1
q^2 migration	...	2.0	2.0
Efficiency	1.2	1.6	1.6
Fit template	$^{+2.3}_{-2.9}$	$^{+1.8}_{-2.4}$	$^{+3.0}_{-3.4}$
Total	$^{+4.0}_{-4.3}$	$^{+4.3}_{-4.5}$	$^{+5.0}_{-5.3}$

$|V_{ub}|$ extraction and relative uncertainties

$$|V_{ub}|/|V_{cb}| = 0.0607 \pm 0.0015\,(\text{stat}) \pm 0.0013\,(\text{syst}) \pm 0.0008\,(D_s) \pm 0.0030\,(\text{FF}) = 0.0607 \pm 0.0037\,(\text{tot})$$

(~2.5%) (~2.1%) (~1.3%) (~4.9%) (~6.1%)

$$|V_{ub}|/|V_{cb}| = 0.0946 \pm 0.0030\,(\text{stat})^{+0.0024}_{-0.0025}\,(\text{syst}) \pm 0.0013\,(D_s) \pm 0.0068\,(\text{FF}) = 0.0946 \pm 0.0079\,(\text{tot})$$

(~3.2%) (~2.6%) (~1.4%) (~7.2%) (~8.4%)

Published $|V_{cb}|$ and $|V_{ub}|$ measurements at LHCb

- At the B factories, $B^{\pm,0}$ decays are used to determine $|V_{cb}|$ and $|V_{ub}|$.

  $|V_{cb}|_{\text{excl.}}$ with $\sim 1.8\,\%$ relative uncertainty based on $\bar{B} \to D^{*} l \bar{\nu}_l$ decays.

  $|V_{ub}|_{\text{excl.}}$ with $\sim 4.1\,\%$ relative uncertainty based on $\bar{B} \to \pi l \bar{\nu}_l$ decays.

[Eur. Phys. J. C 74, 3026]

[Phys. Rev. D107, 052008]

- LHCb has a **unique opportunity for using exclusive Λ_b^0 and B_s^0 semileptonic channels** to determine $|V_{cb}|$ and $|V_{ub}|$.

  → Potentially subject to **different sources of uncertainties** wrt. $B^{\pm,0}$ decays.

  → B_s^0 is theoretically advantageous wrt. $B^{\pm,0}$ as the heavier s quark allows for **more precise LQCD calculations**.

Some examples..

[Phys. Rev. D 99, 114512 (2019)]
[Phys. Rev. D 97, 054502 (2018)]
[Phys. Rev. D 91.7 (2015)]

>> Next, a comprehensive summary of LHCb measurements concerning $|V_{cb}|$ and $|V_{ub}|$..

Operation and data

$$\sqrt{s} = 7\,\mathrm{TeV} : \sigma(pp \rightarrow b\bar{b}X) = (72.0 \pm 0.3 \pm 6.8)\,\mu b$$

$$\sqrt{s} = 13\,\mathrm{TeV} : \sigma(pp \rightarrow b\bar{b}X) = (144 \pm 1 \pm 21)\,\mu b$$